Supplementary Information

Picolinic acid based acyclic bifunctional chelating agent and its methionine conjugate as potential SPECT imaging agents: Syntheses and preclinical evaluation

K Ganesh Kadiyala,[a,b] Tulika Tyagi,[a] Dipti Kakkar,[a] Nidhi Chadha,[a,b] Krishna Chuttani,[a] Bal Gangadhar Roy,[a] Meganathan Thirumal,[b] Anil K. Mishra,[*a] Anupama Datta.[*a]

[a] Division of Cyclotron and Radiopharmaceutical Sciences, Institute of Nuclear Medicine and Allied Sciences, Defence Research and Development Organization, Brig S. K. Mazumdar Marg, Delhi-110054, India.

[b] Department of Chemistry, University of Delhi, Delhi-110007, India.

[*] To whom correspondence should be addressed. Tel: +91-11-23905123, 23905117

e-mail: anupama@inmas.drdo.in or akmishra63@gmail.com

Contents

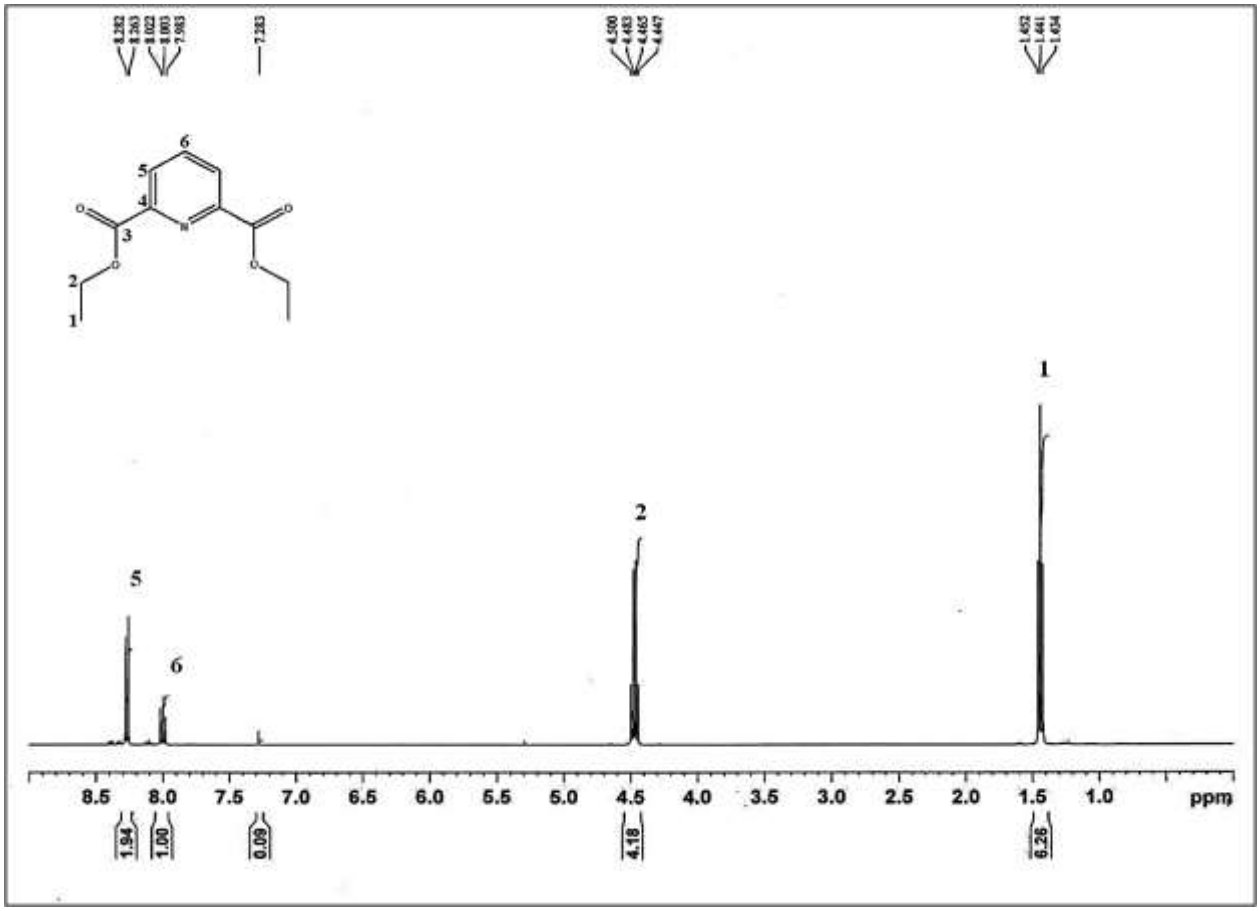

Figure S1. ^{1}H NMR spectrum of diethyl pyridine-2,6-di carboxylate **(2)**

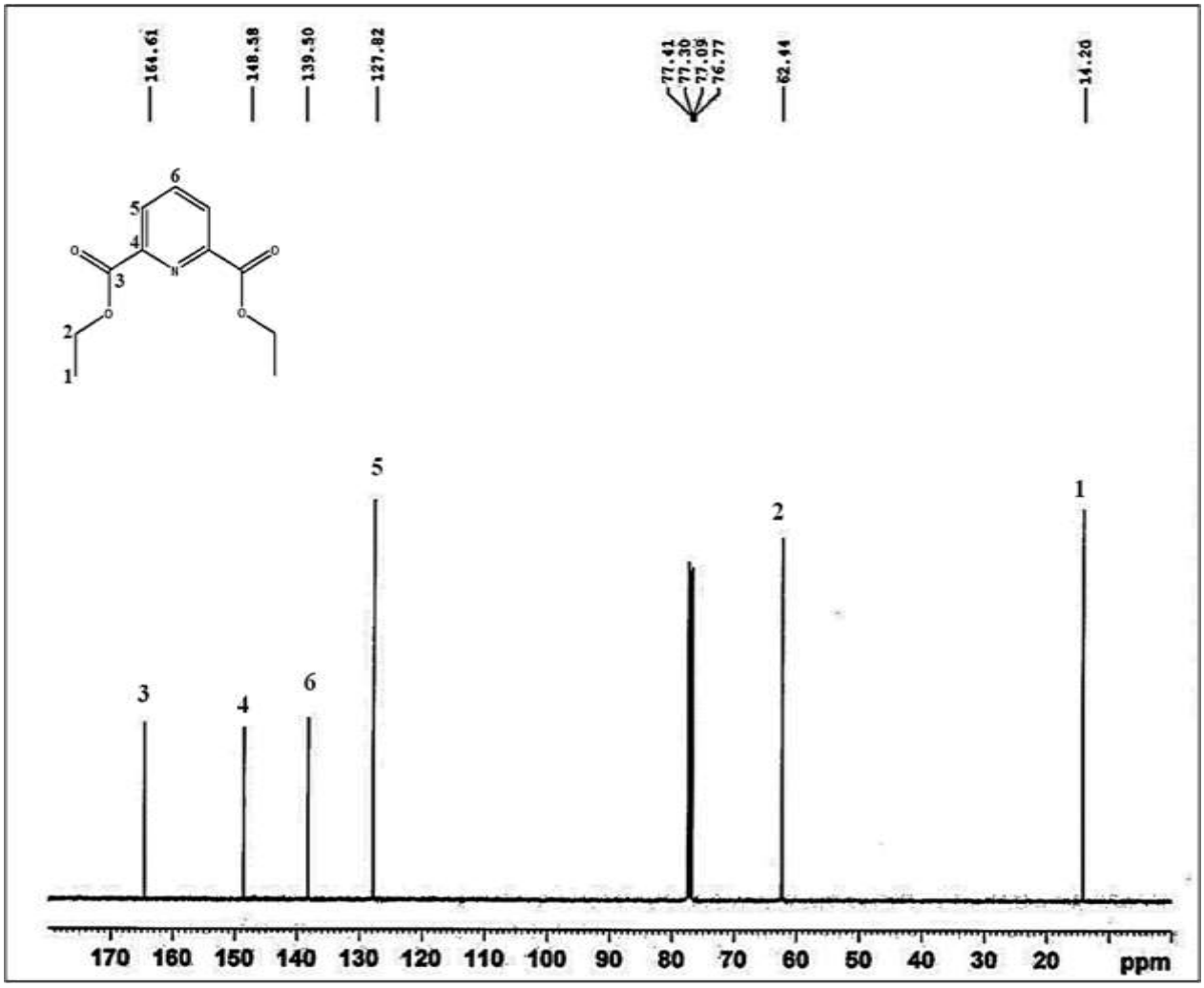

Figure S2. ^{13}C NMR spectrum of diethyl pyridine-2,6-di carboxylate **(2)**

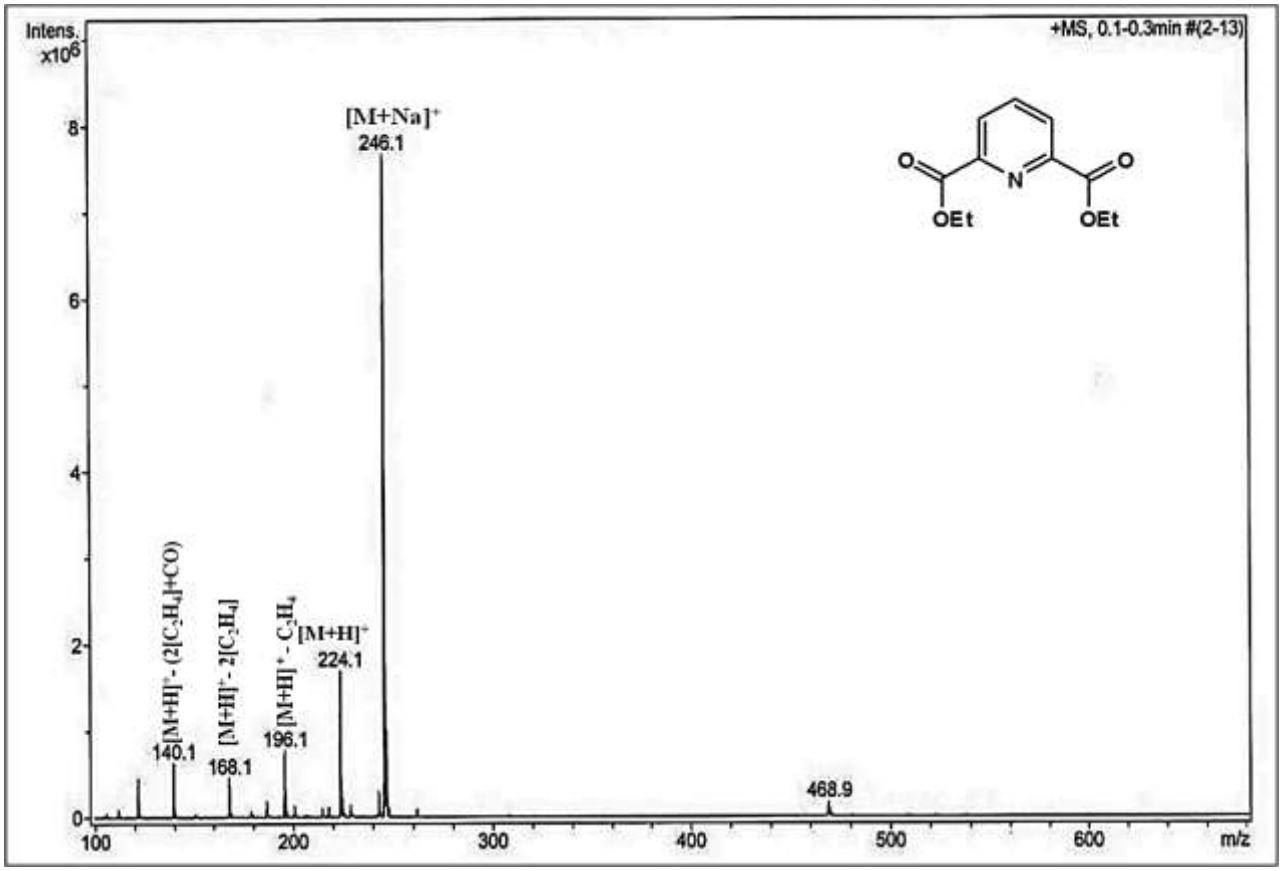

Figure S3. Mass spectrum of diethyl pyridine-2,6-di carboxylate **(2)**

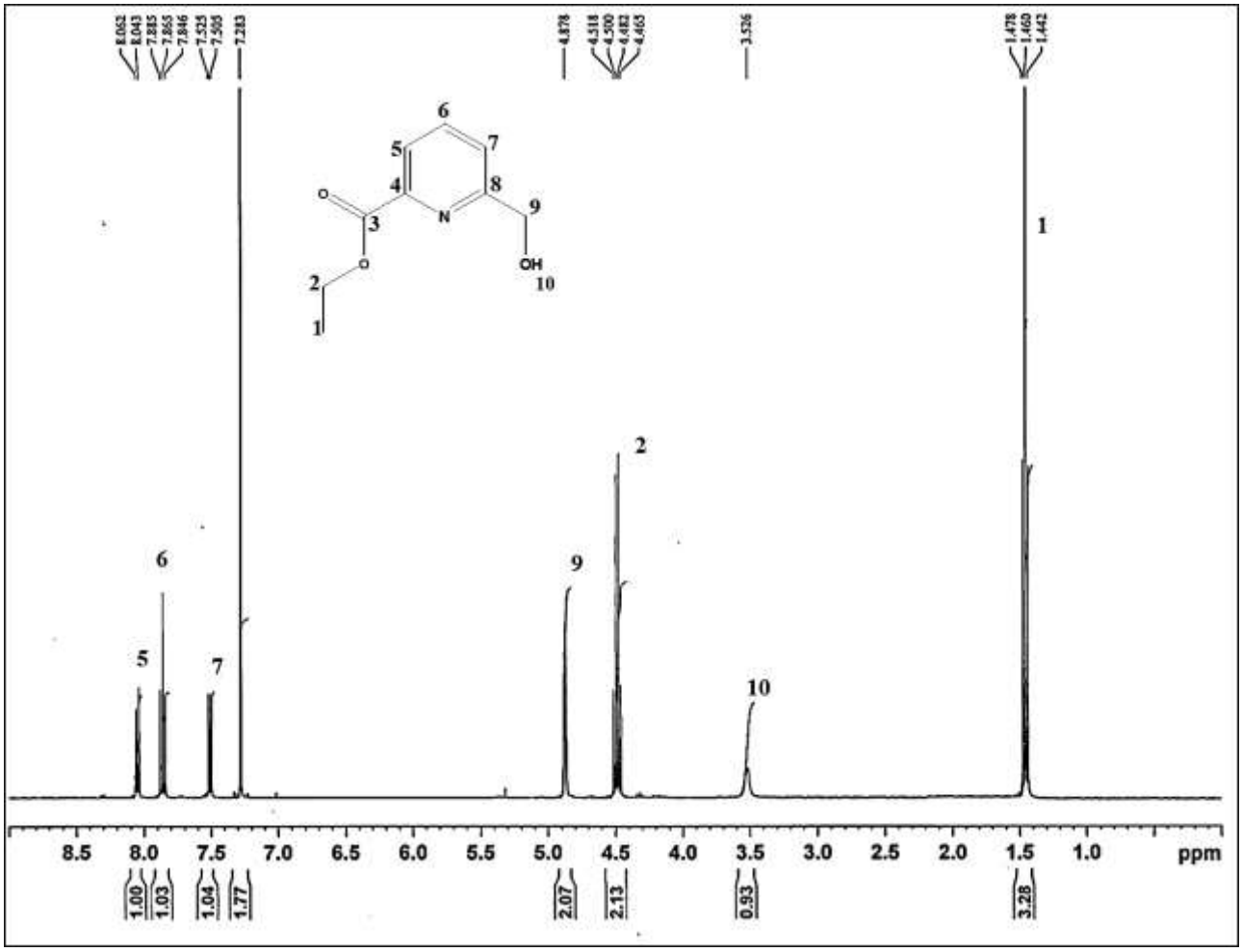

Figure S4. ^{1}H NMR spectrum of ethyl 6-(hydroxylmethyl)picolinate **(3)**

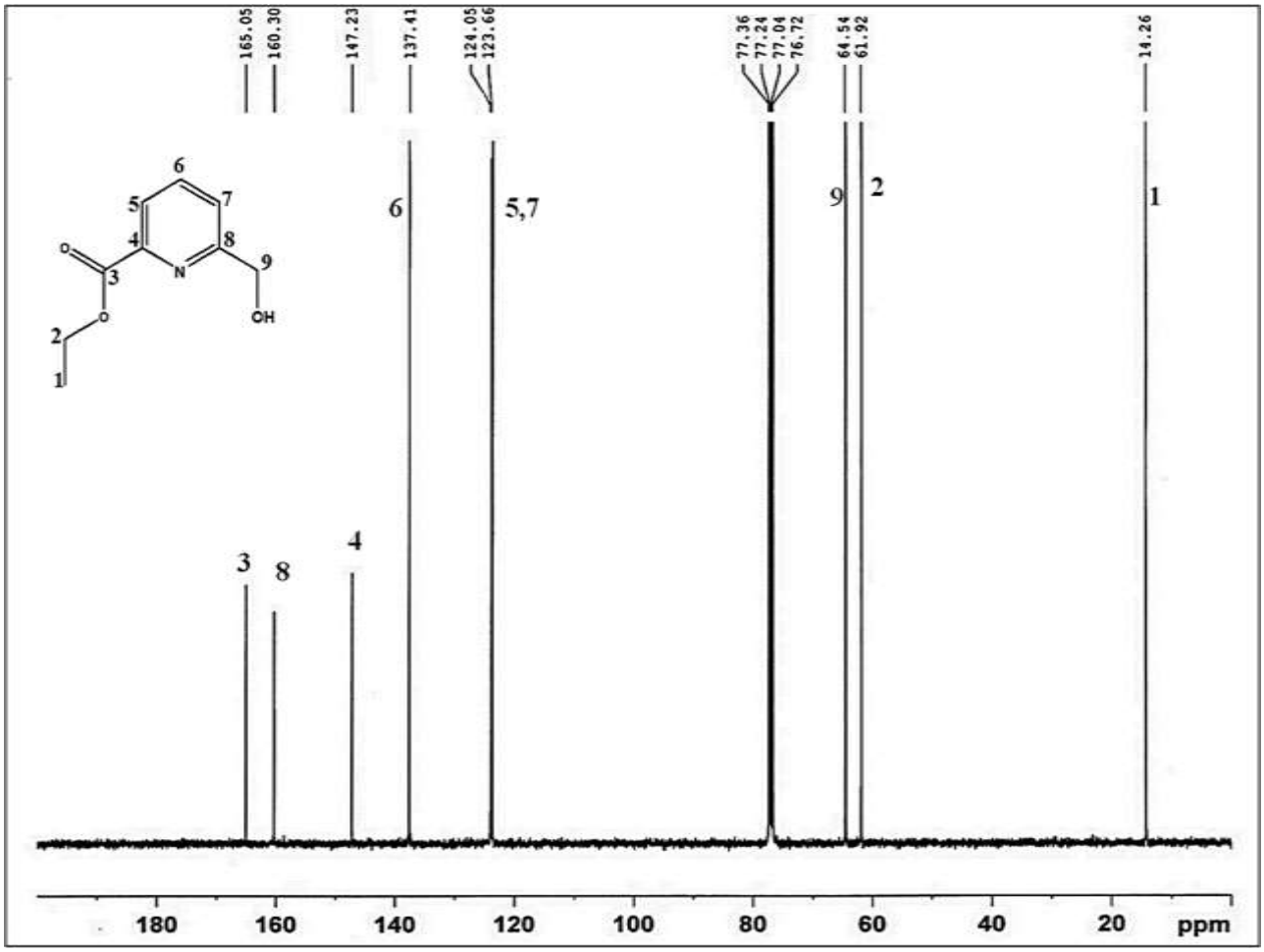

Figure S5. ^{13}C NMR spectrum of ethyl 6-(hydroxylmethyl)picolinate **(3)**

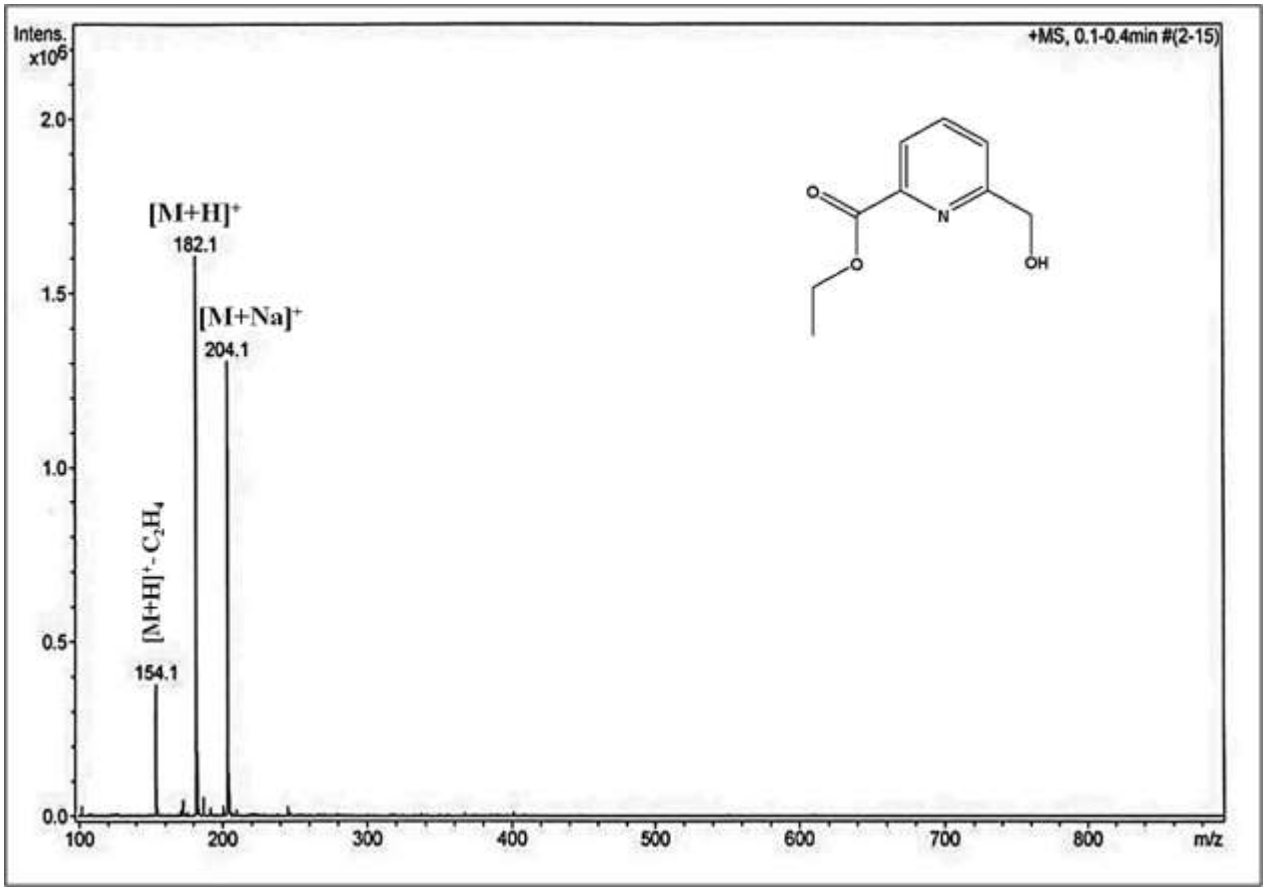

Figure S6. Mass spectrum ethyl 6-(hydroxylmethyl)picolinate **(3)**

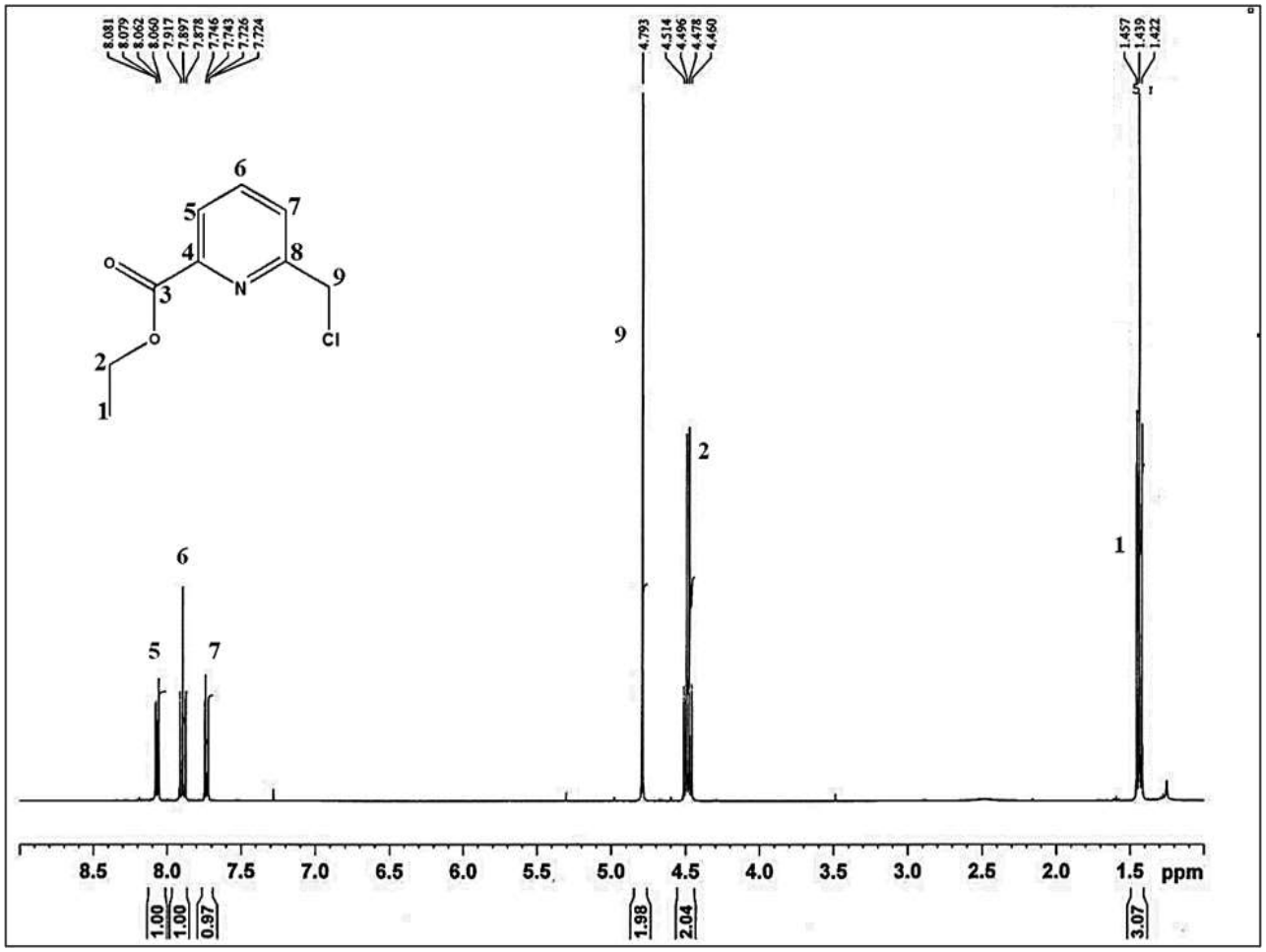

Figure S7. ^{1}H NMR spectrum of ethyl 6-(chloromethyl)picolinate **(4)**

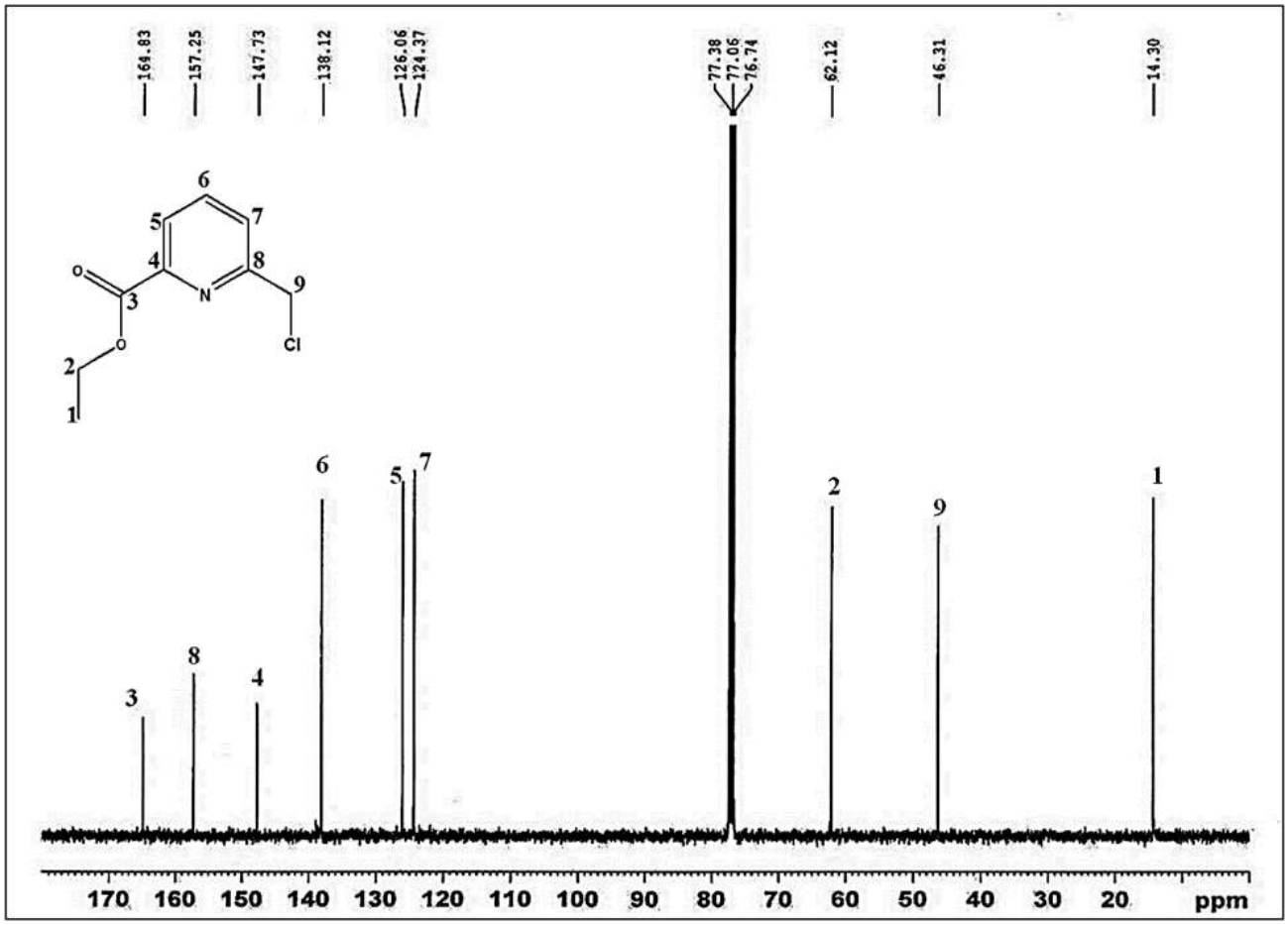

Figure S8. ^{13}C NMR spectrum of ethyl 6-(chloromethyl)picolinate **(4)**

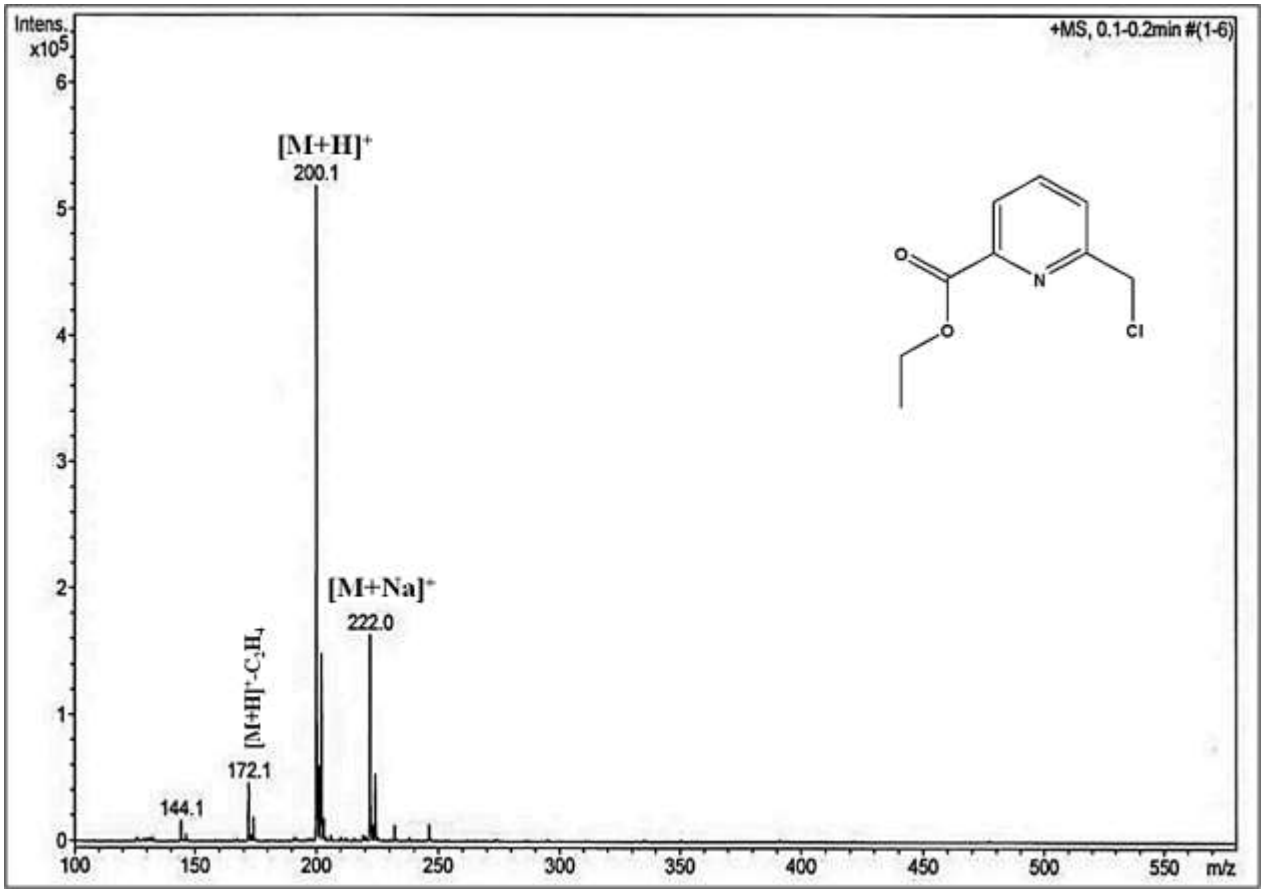

Figure S9. Mass spectrum of ethyl 6-(chloromethyl)picolinate **(4)**

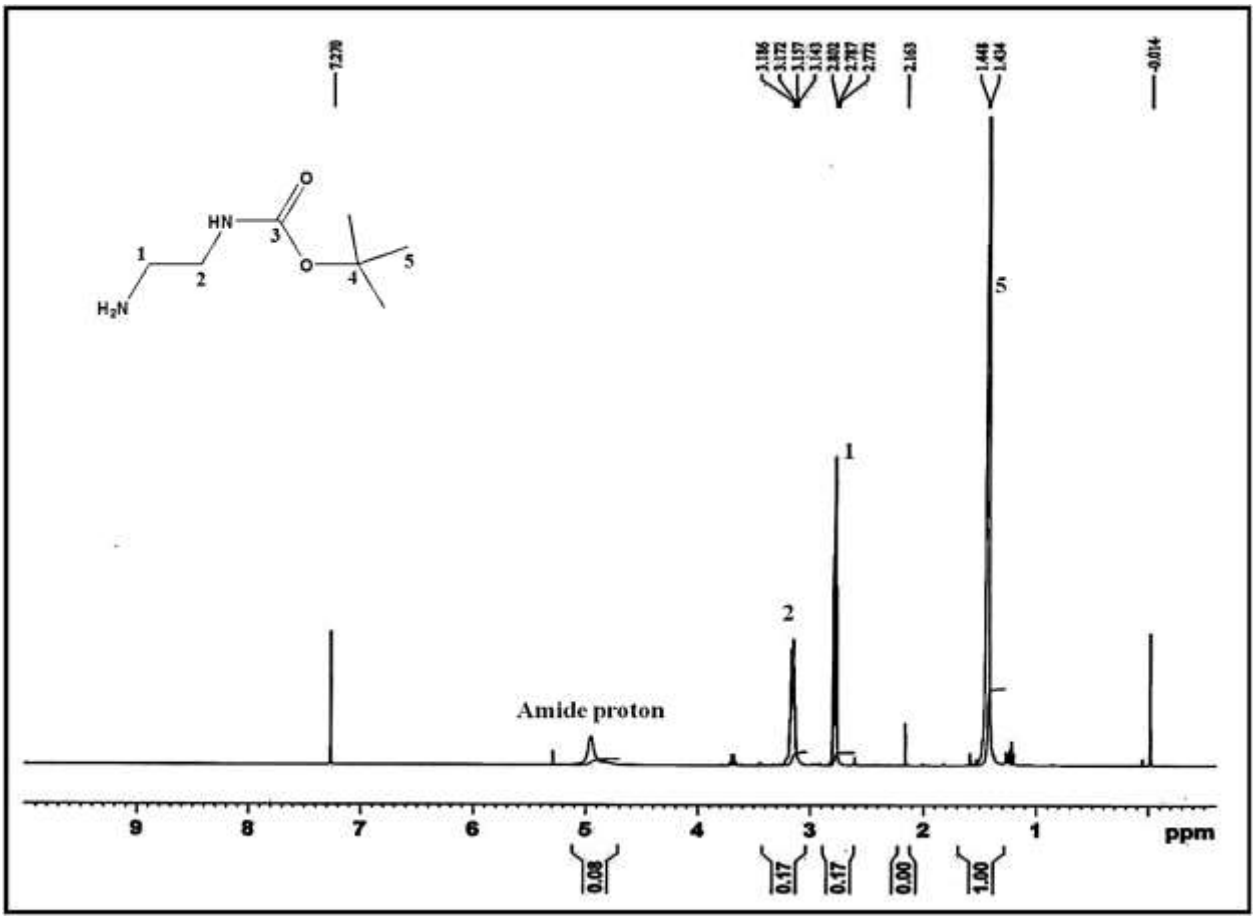

Figure S10. ^{1}H NMR spectrum of *tert*-butyl 2-aminoethylcarbamate **(6)**

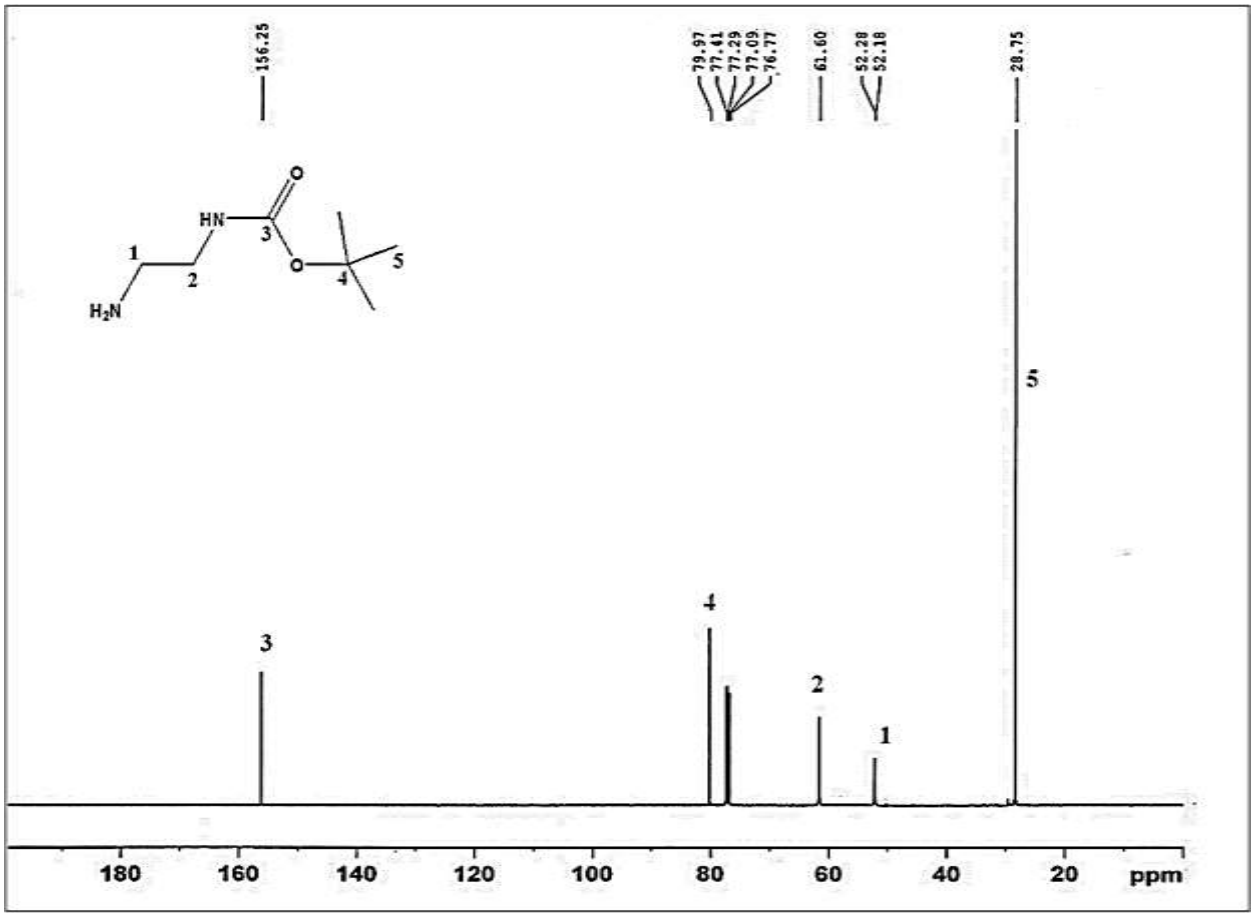

Figure S11. ^{13}C NMR spectrum of *tert*-butyl 2-aminoethylcarbamate **(6)**

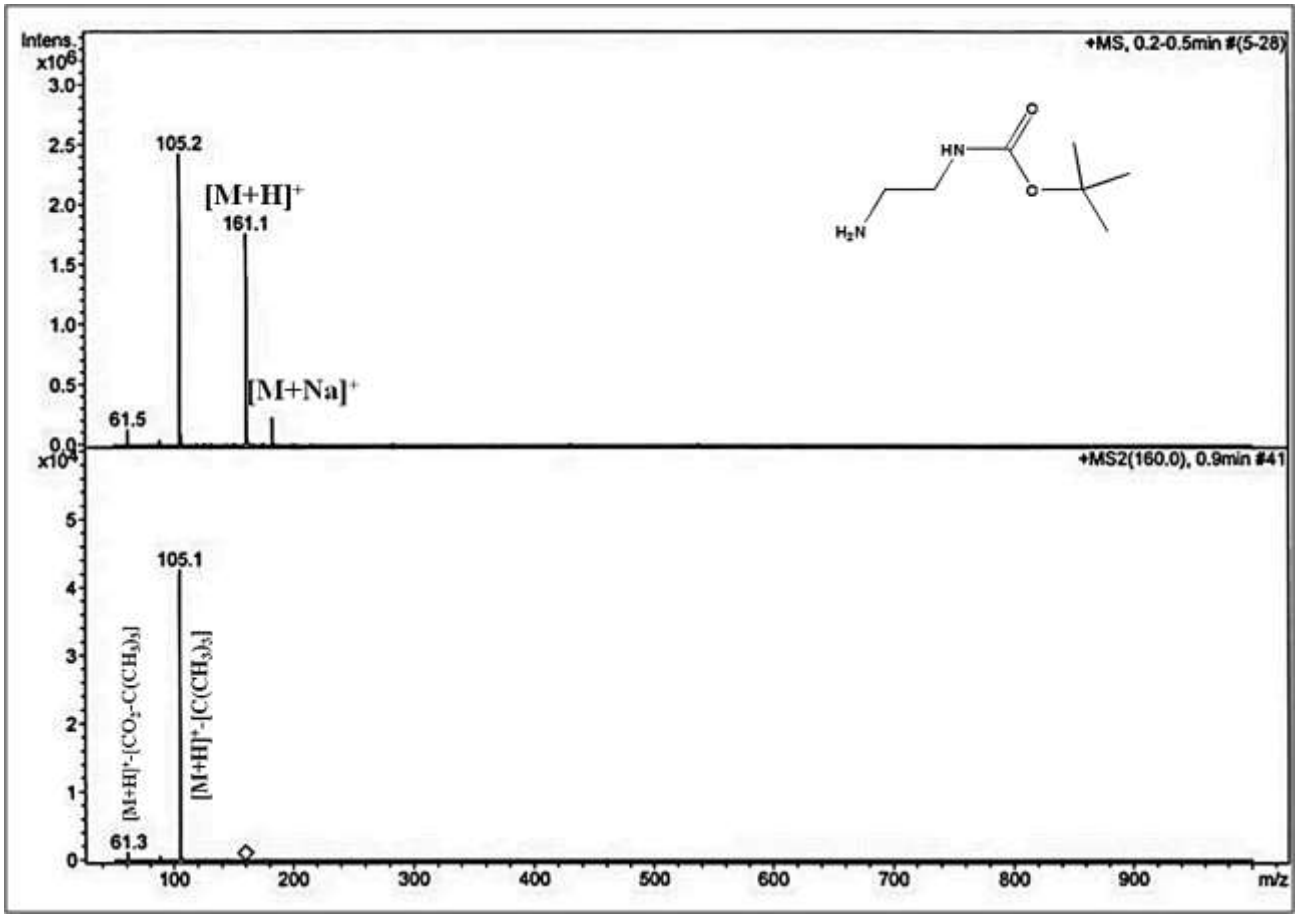

Figure S12. Mass spectrum *tert*-butyl 2-aminoethylcarbamate **(6)**

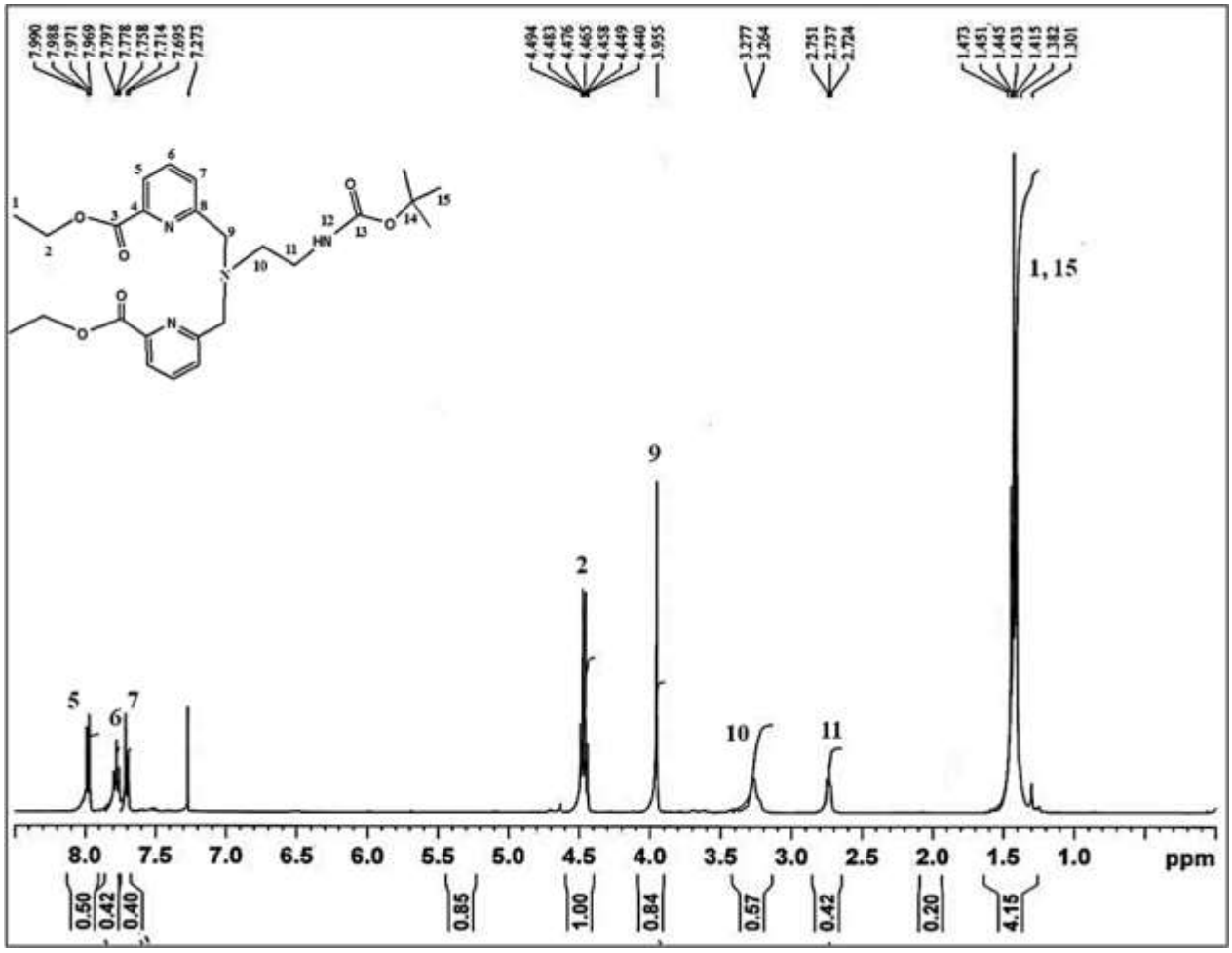

Figure S13. ^{1}H NMR spectrum of

diethyl 6,6′-(2(*tert*-butoxycarbonylamino)ethylazanediyl)bis(methylene)dipicolinate **(7)**

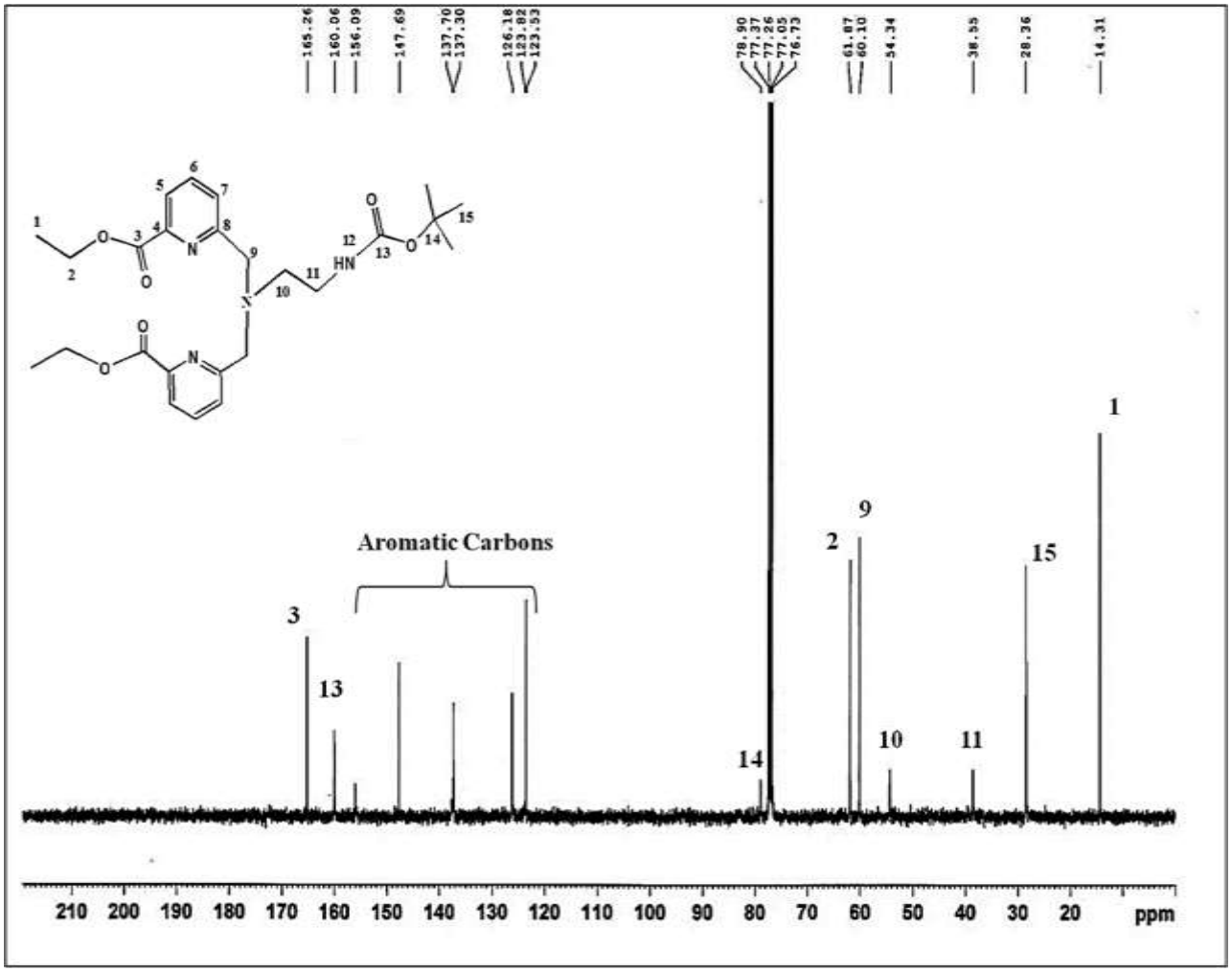

Figure S14. ^{13}C NMR spectrum of

diethyl 6,6′-(2(*tert*-butoxycarbonylamino)ethylazanediyl)bis(methylene)dipicolinate **(7)**

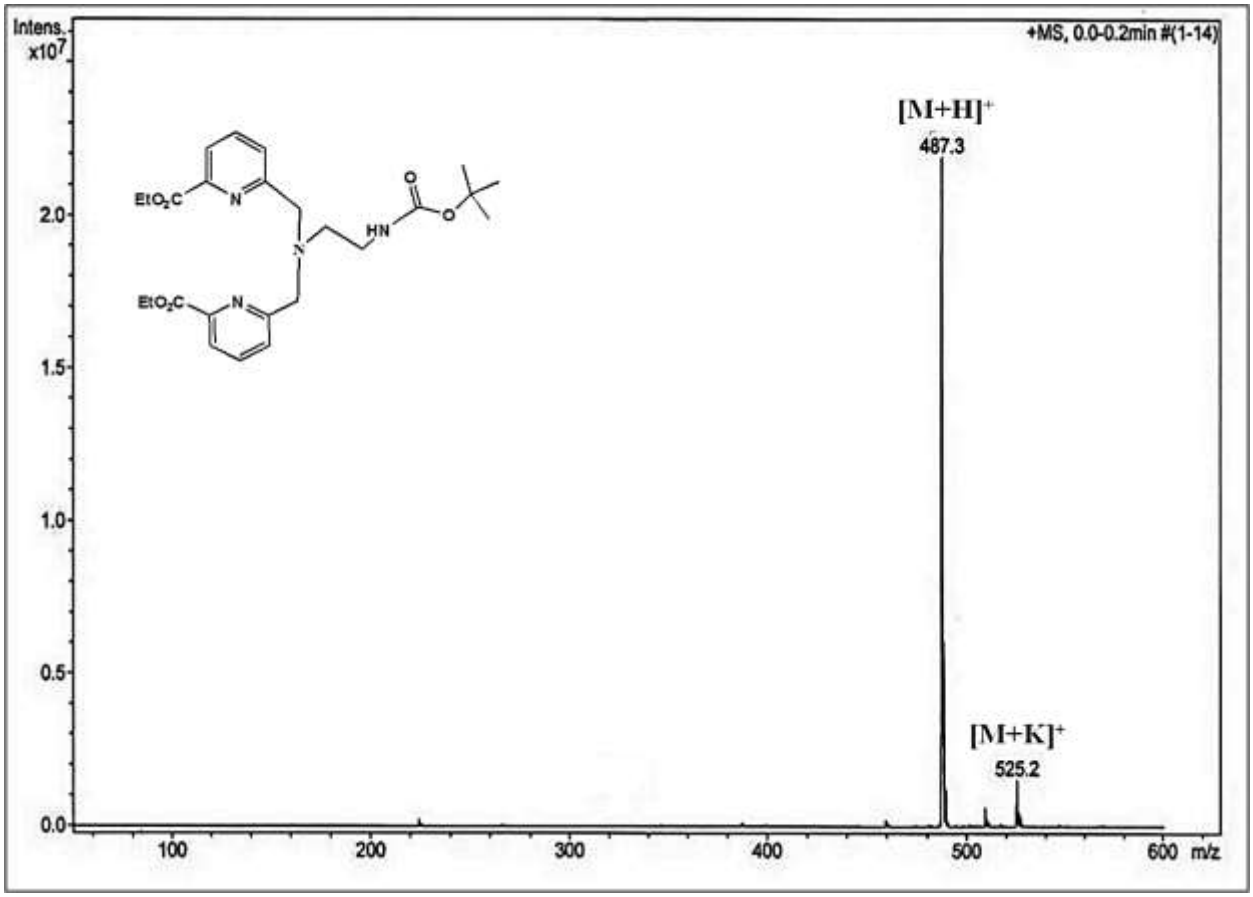

Figure S15. Mass spectrum of

diethyl 6,6′-(2(*tert*-butoxycarbonylamino)ethylazanediyl)bis(methylene)dipicolinate **(7)**

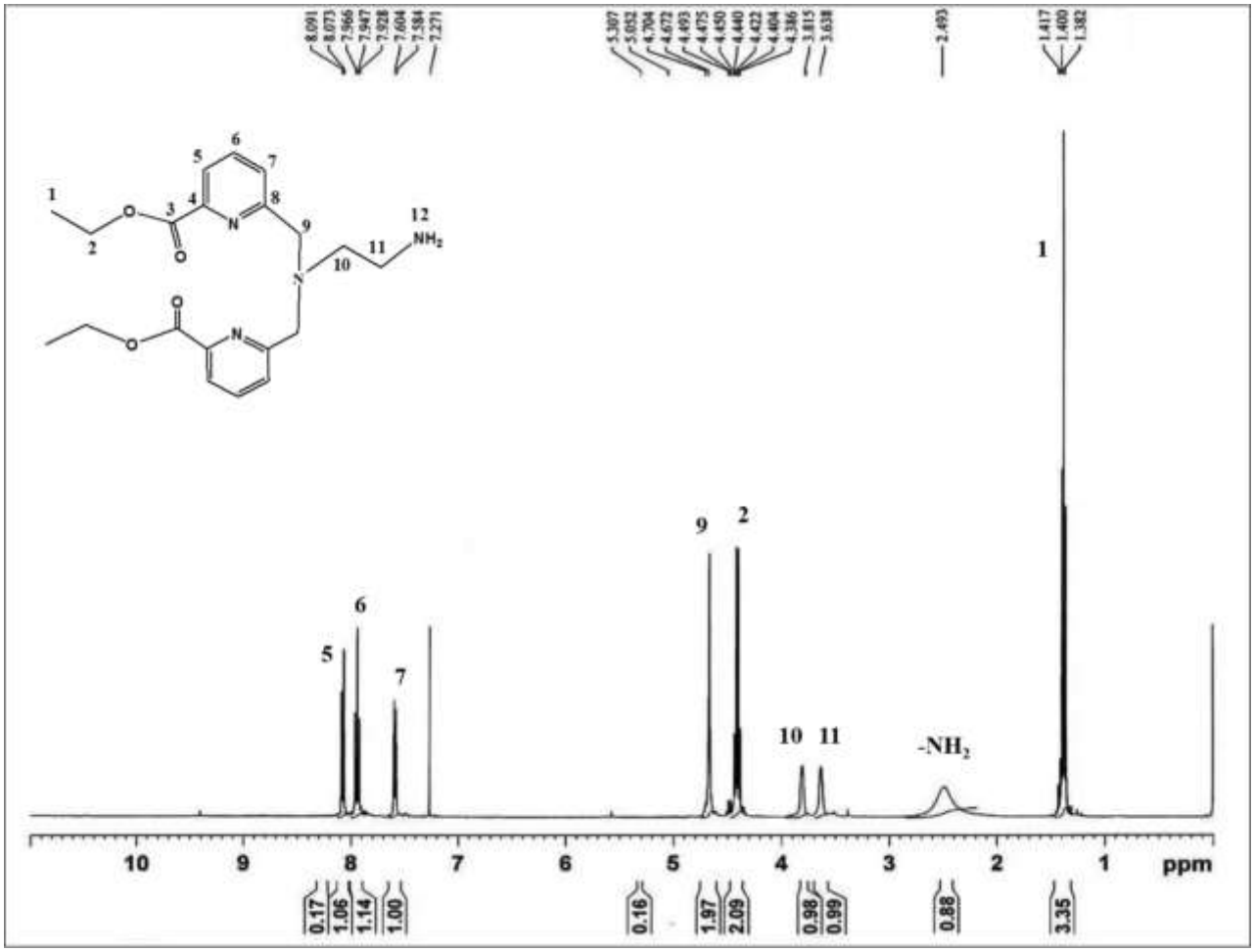

Figure S16. ^{1}H NMR spectrum of

diethyl 6,6′-(2-aminoethylazanediyl)bis(methylene)dipicolinate **(8)**

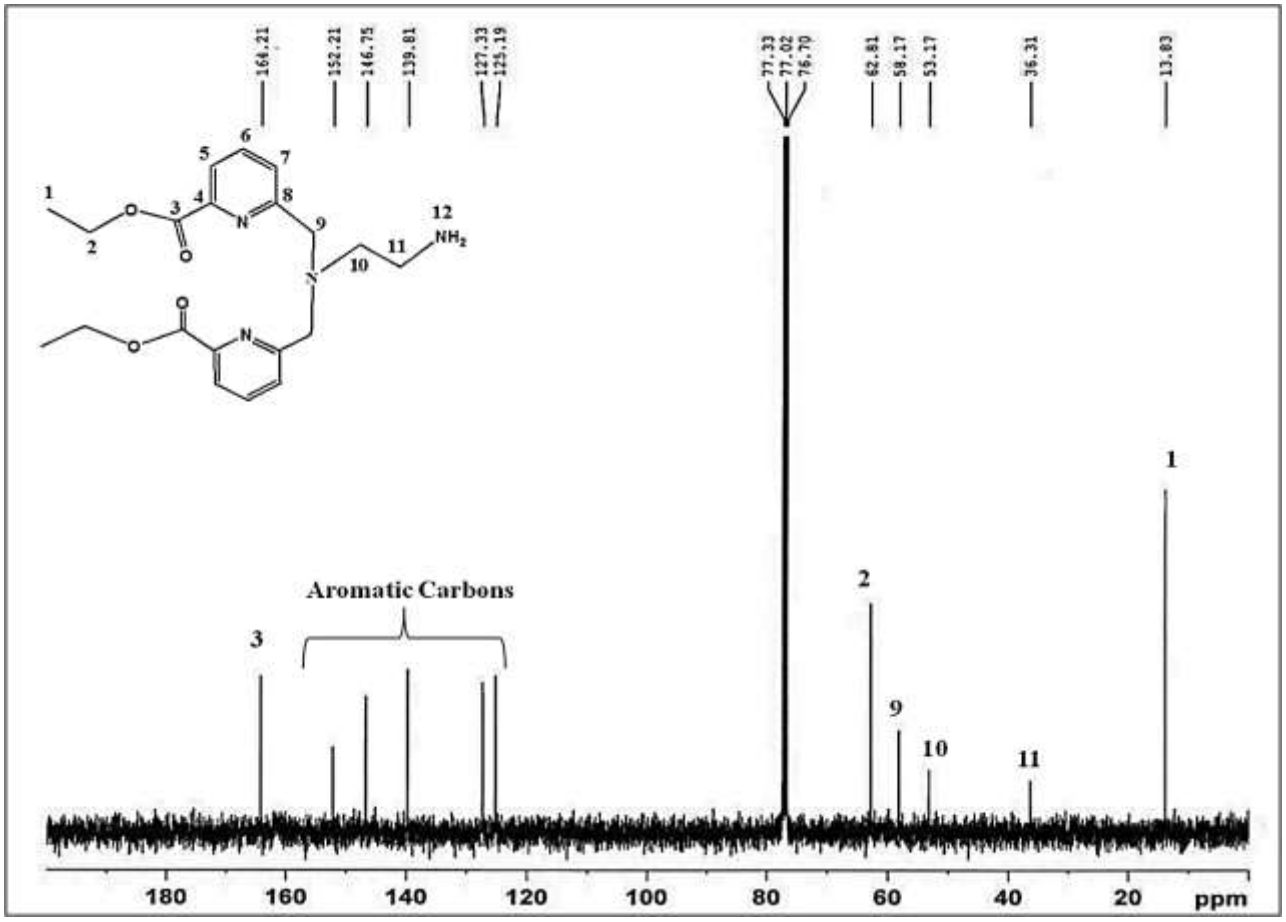

Figure S17. ^{13}C NMR spectrum of

diethyl 6,6′-(2-aminoethylazanediyl)bis(methylene)dipicolinate **(8)**

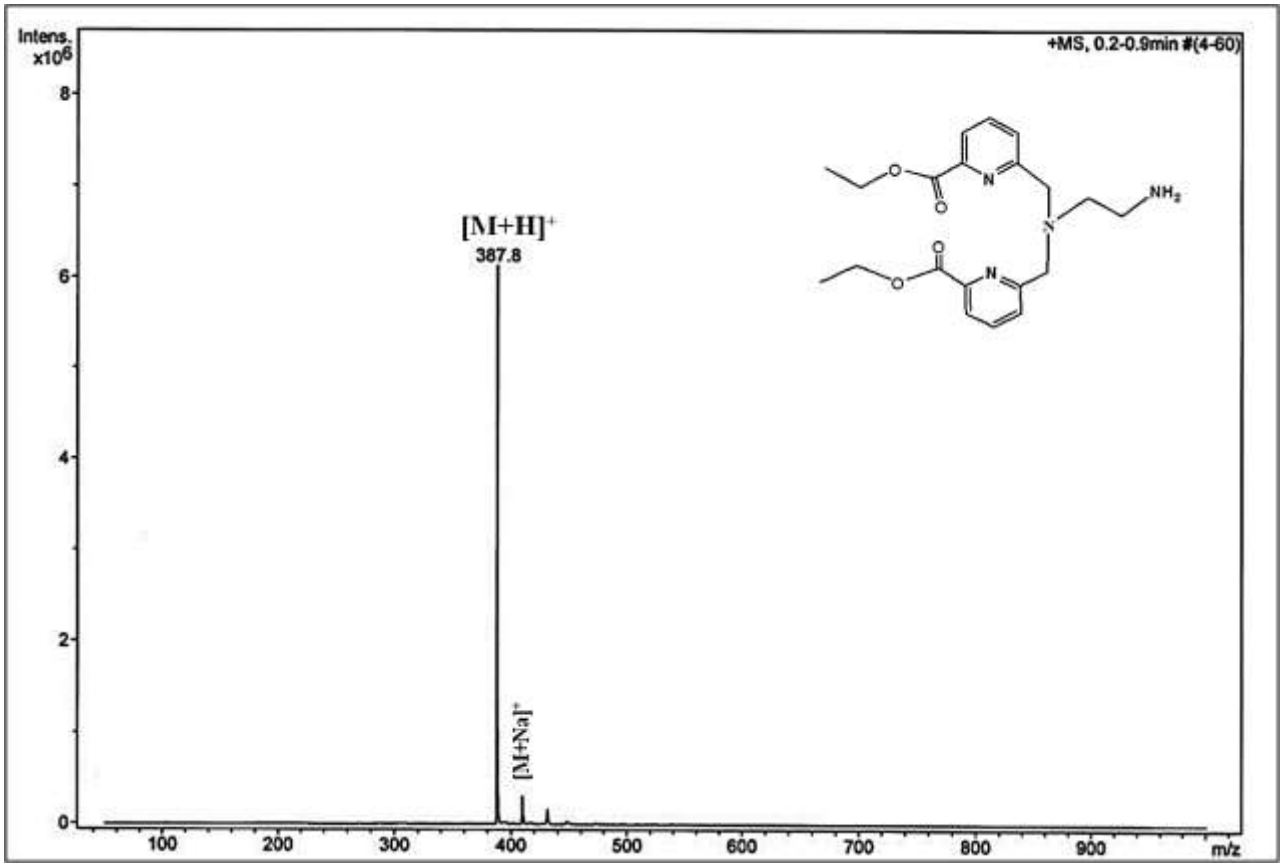

Figure S18. Mass spectrum of

diethyl 6,6′-(2-aminoethylazanediyl)bis(methylene)dipicolinate **(8)**

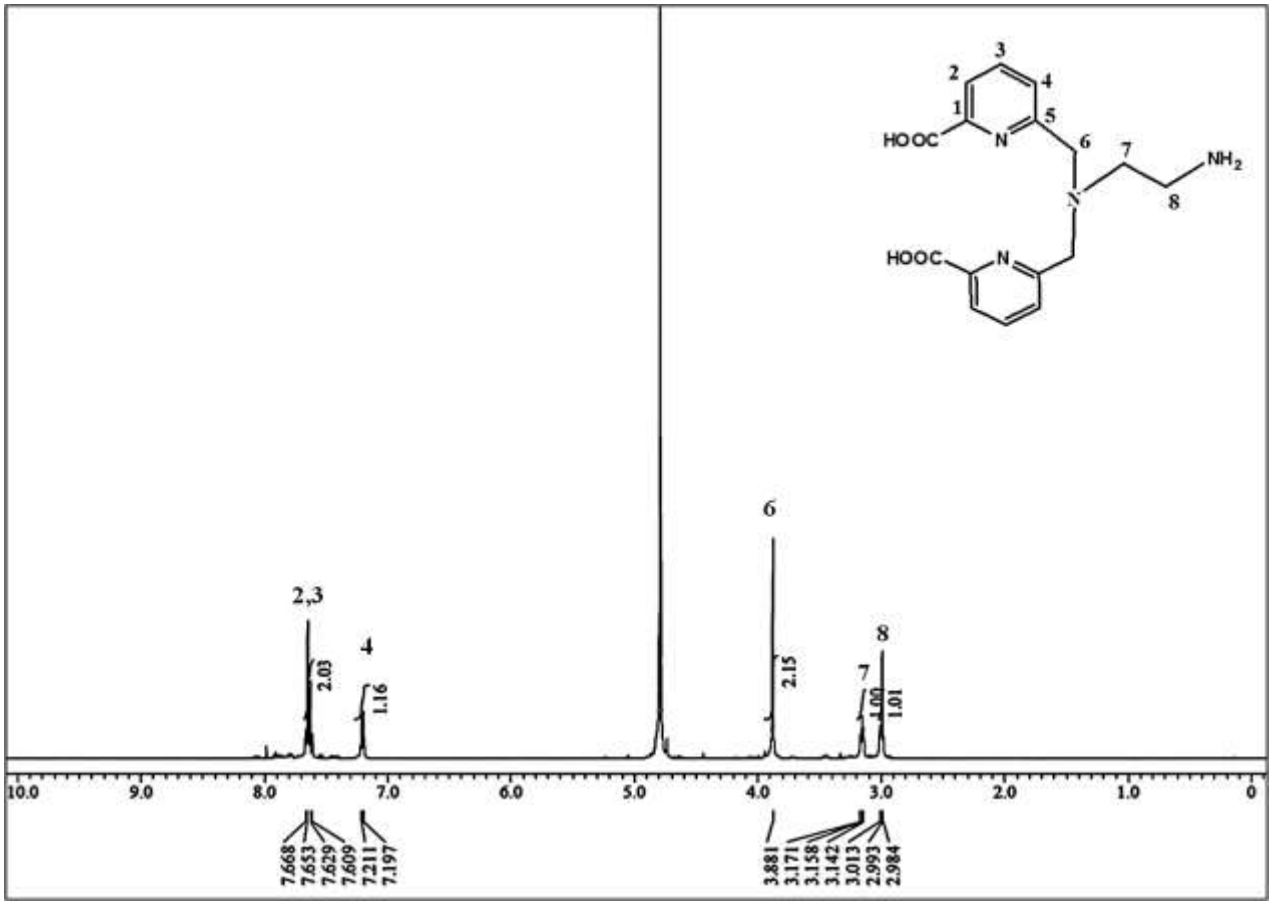

Figure S19. ^{1}H NMR spectrum of 6,6'-(2-aminoethylazanediyl)bis(methylene)dipicolinic acid (**H_2pentapa-en-NH_2**)

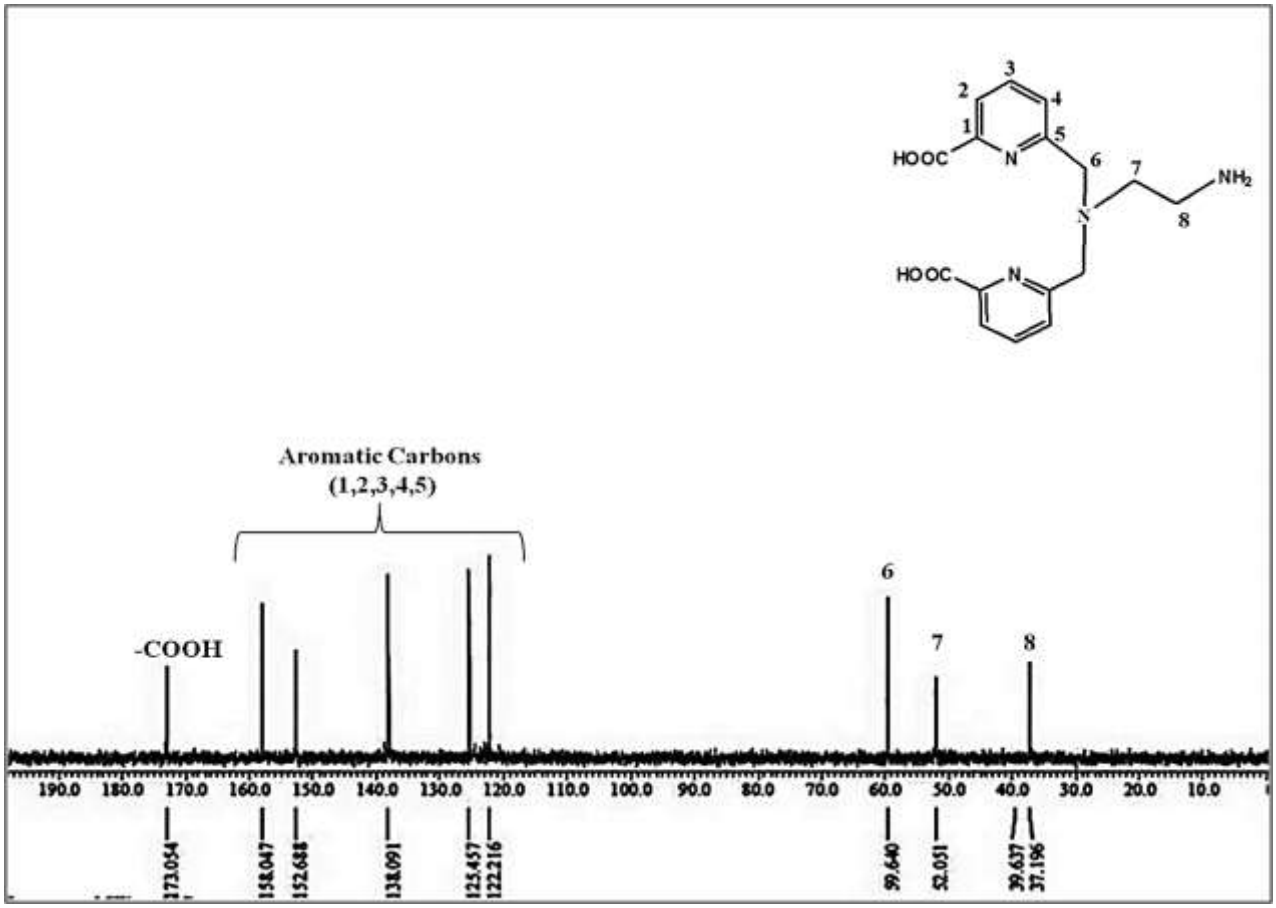

Figure S20. ^{13}C NMR spectrum of 6,6'-(2-aminoethylazanediyl)bis(methylene)dipicolinic acid (**H_2pentapa-en-NH_2**)

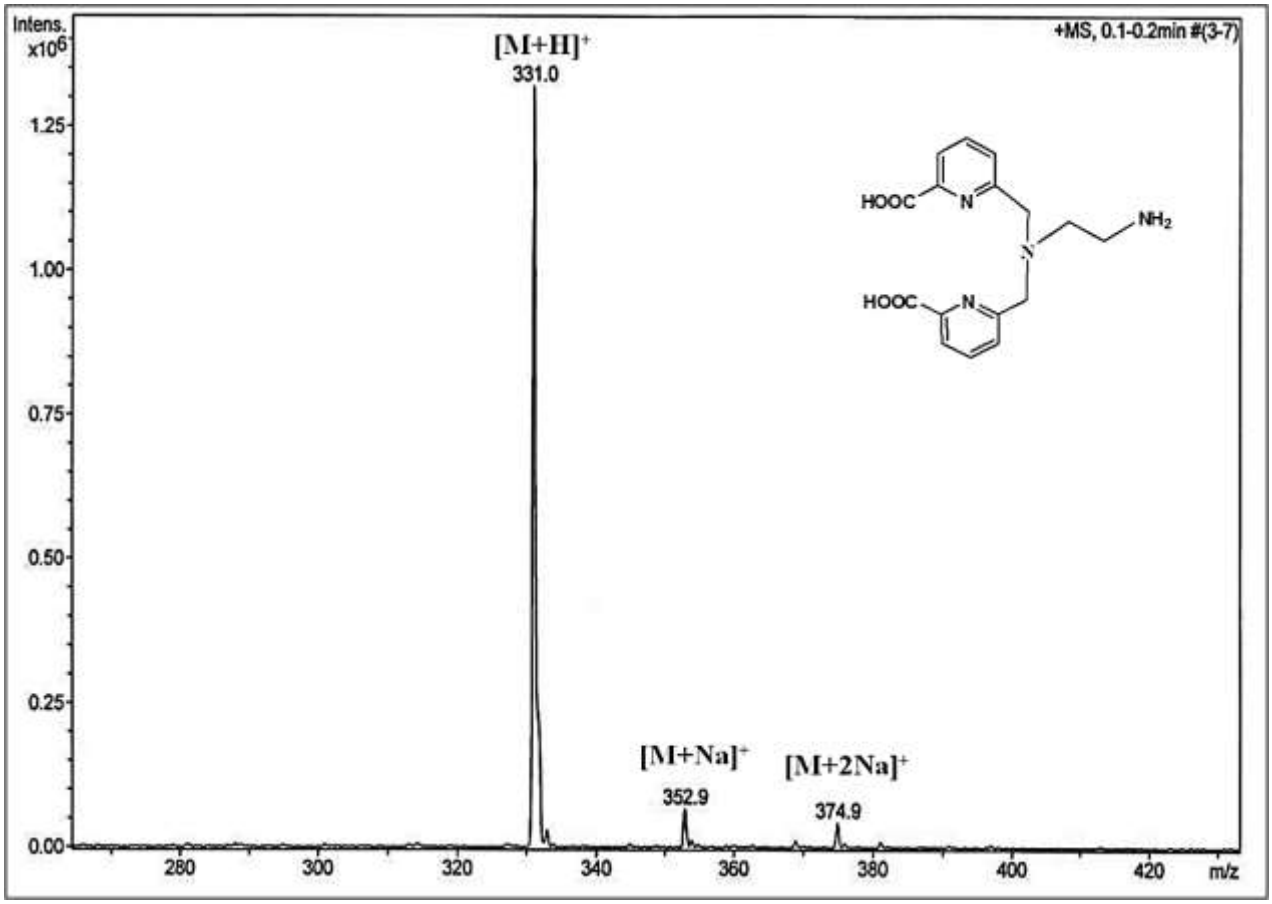

Figure S21. Mass spectrum of 6,6'-(2-aminoethylazanediyl)bis(methylene)dipicolinic acid (**H_2pentapa-en-NH_2**)

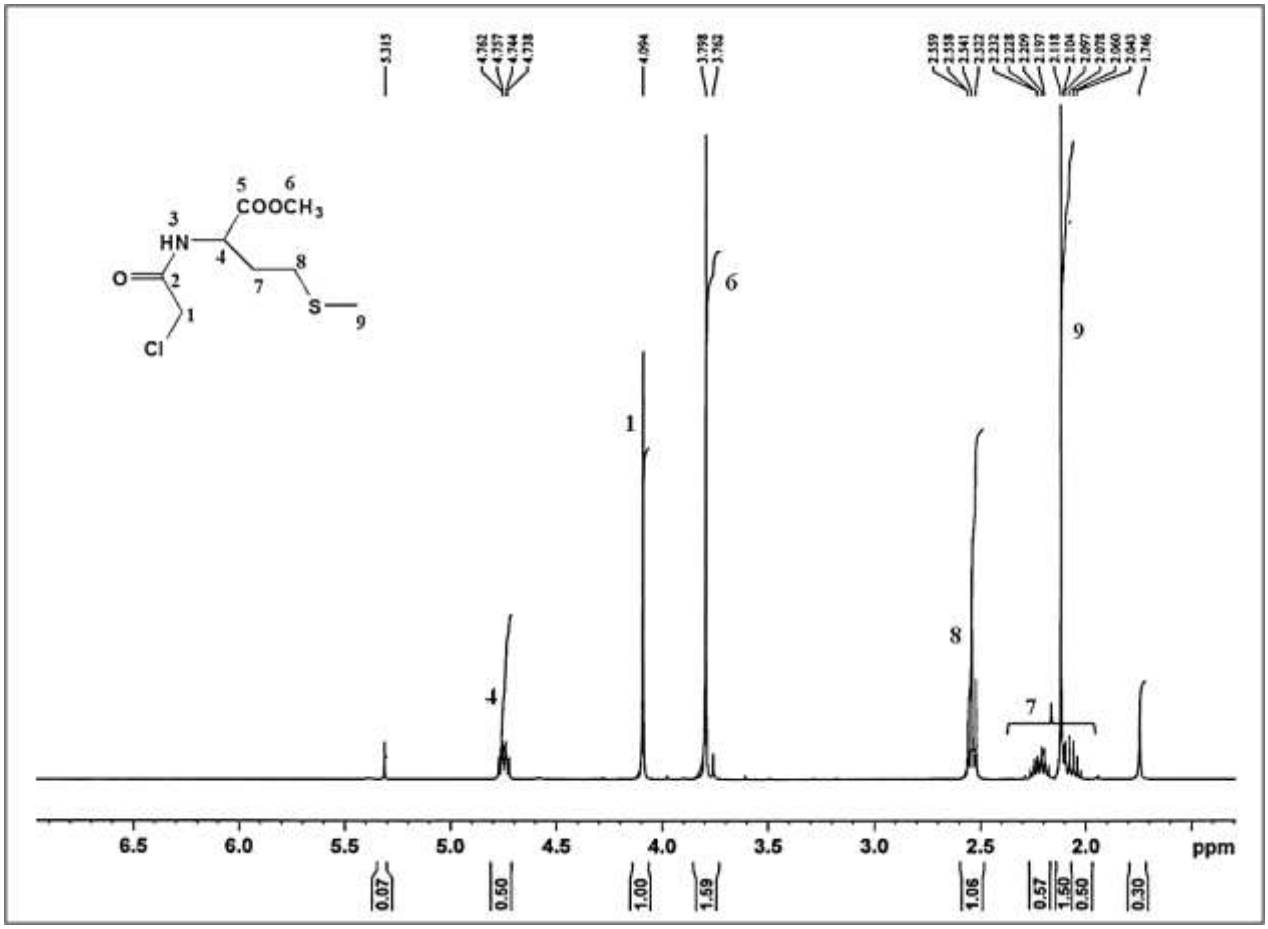

Figure S22. ^{1}H NMR spectrum of methyl 2-(2-chloroacetamido-4-(methylthio)butanoate **(10)**

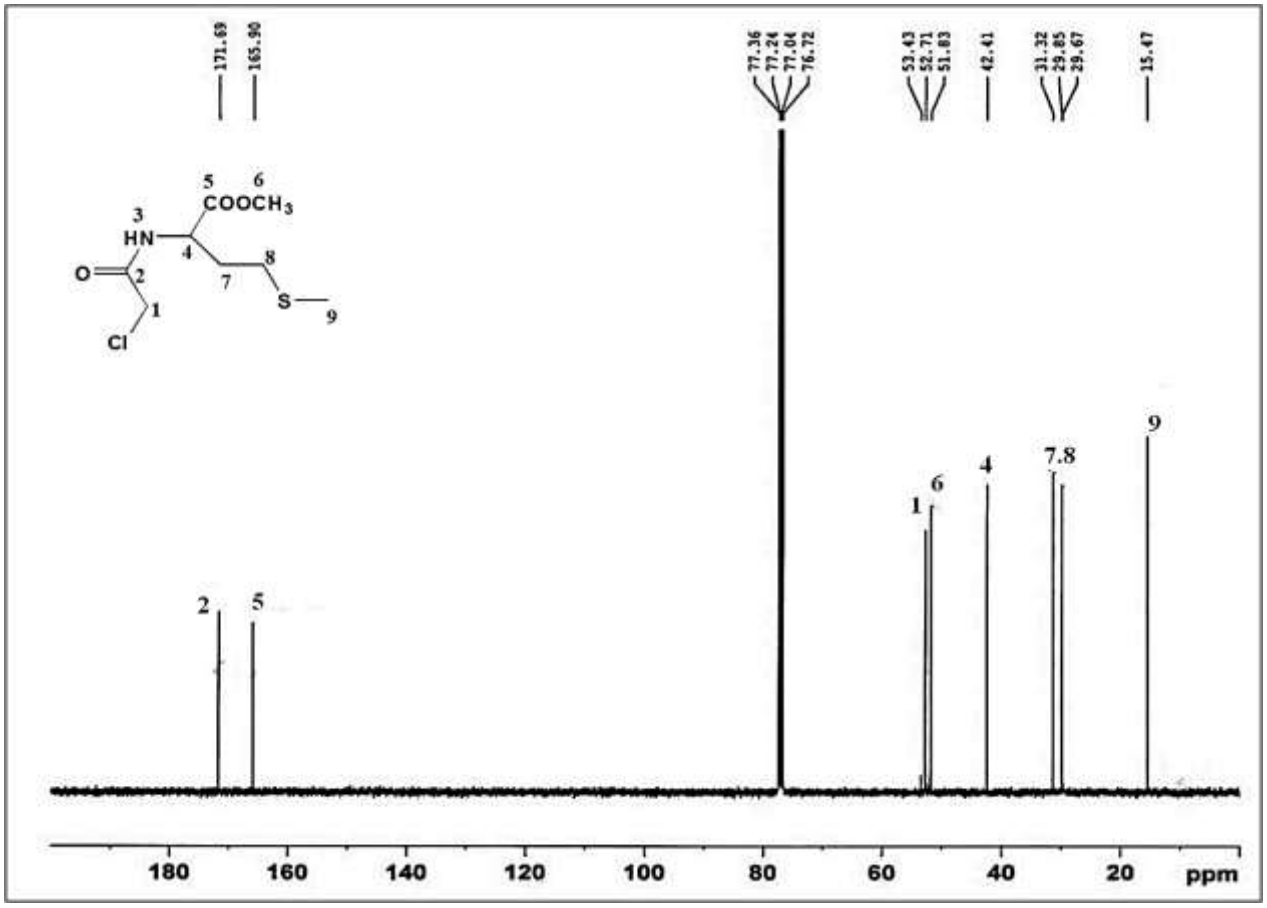

Figure S23. ^{13}C NMR spectrum of methyl 2-(2-chloroacetamido-4-(methylthio)butanoate **(10)**

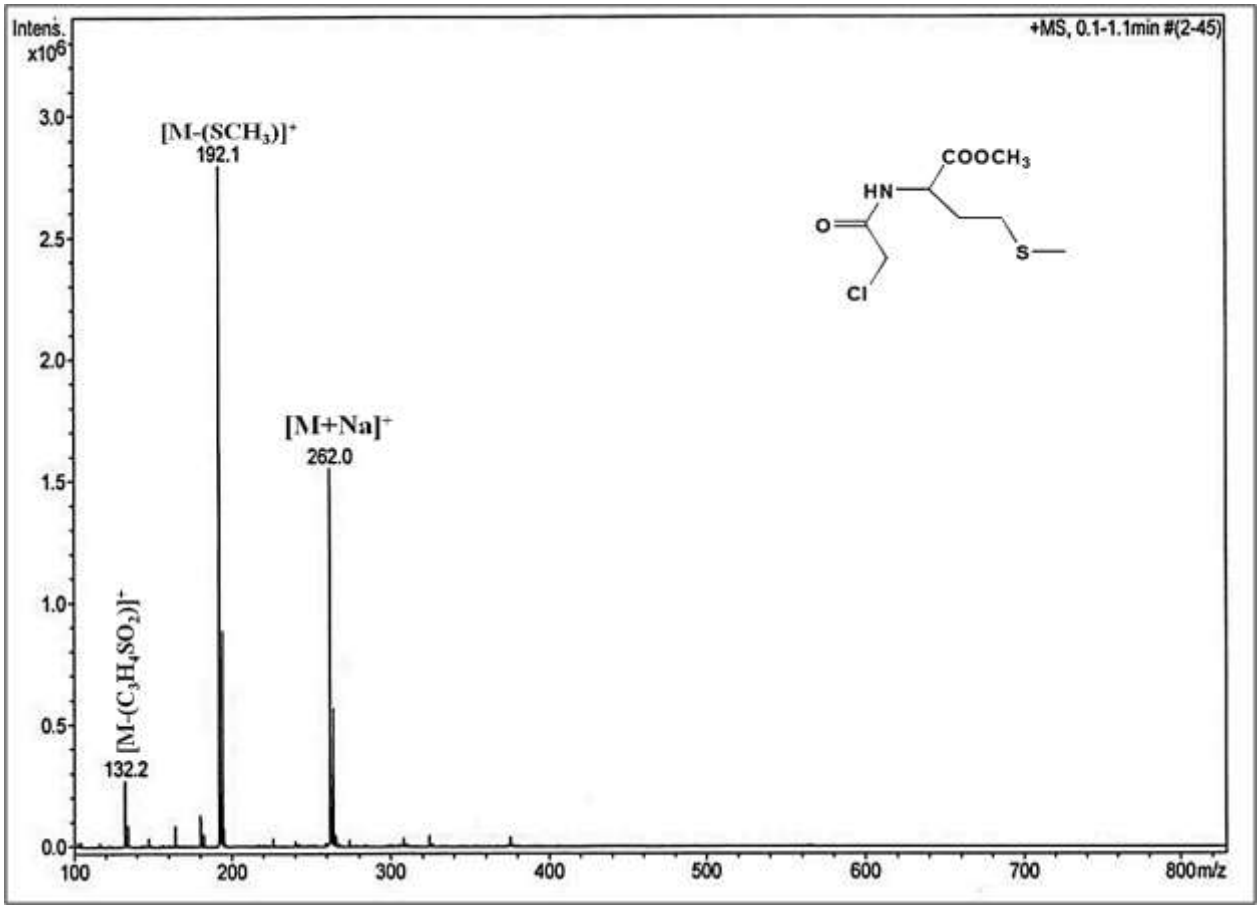

Figure S24. Mass spectrum of methyl 2-(2-chloroacetamido-4-(methylthio)butanoate **(10)**

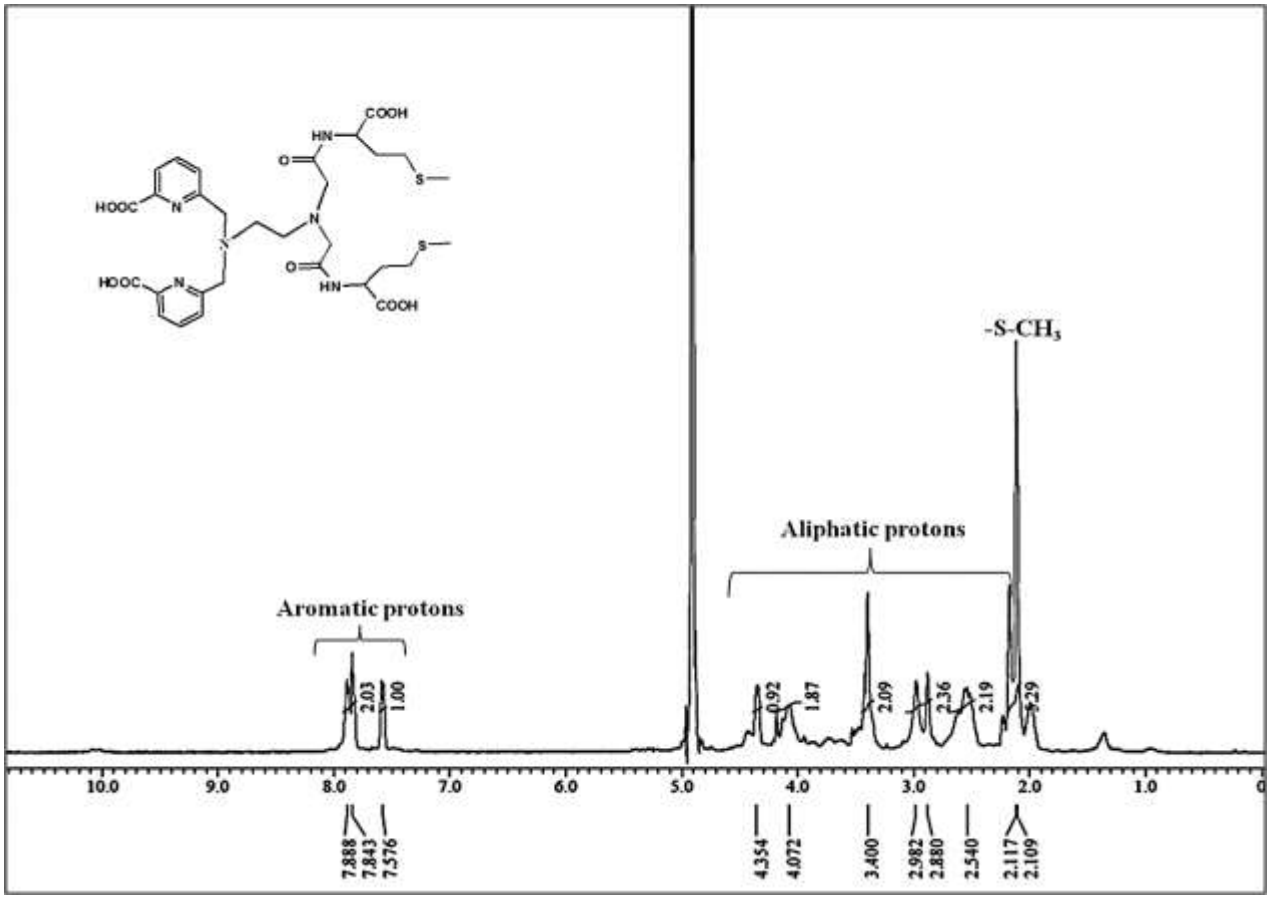

Figure S25. ^{1}H NMR spectrum of 6-(9-carboxy-5-(1-carboxy-3-(methylthio) propylamino)-2-oxoethyl)-2((6-carboxypyridin-2-yl)methyl)-7-oxo-12thia-2,5,8-triazatridecyl)picolonic acid (**H_2pentapa-en-met$_2$**)

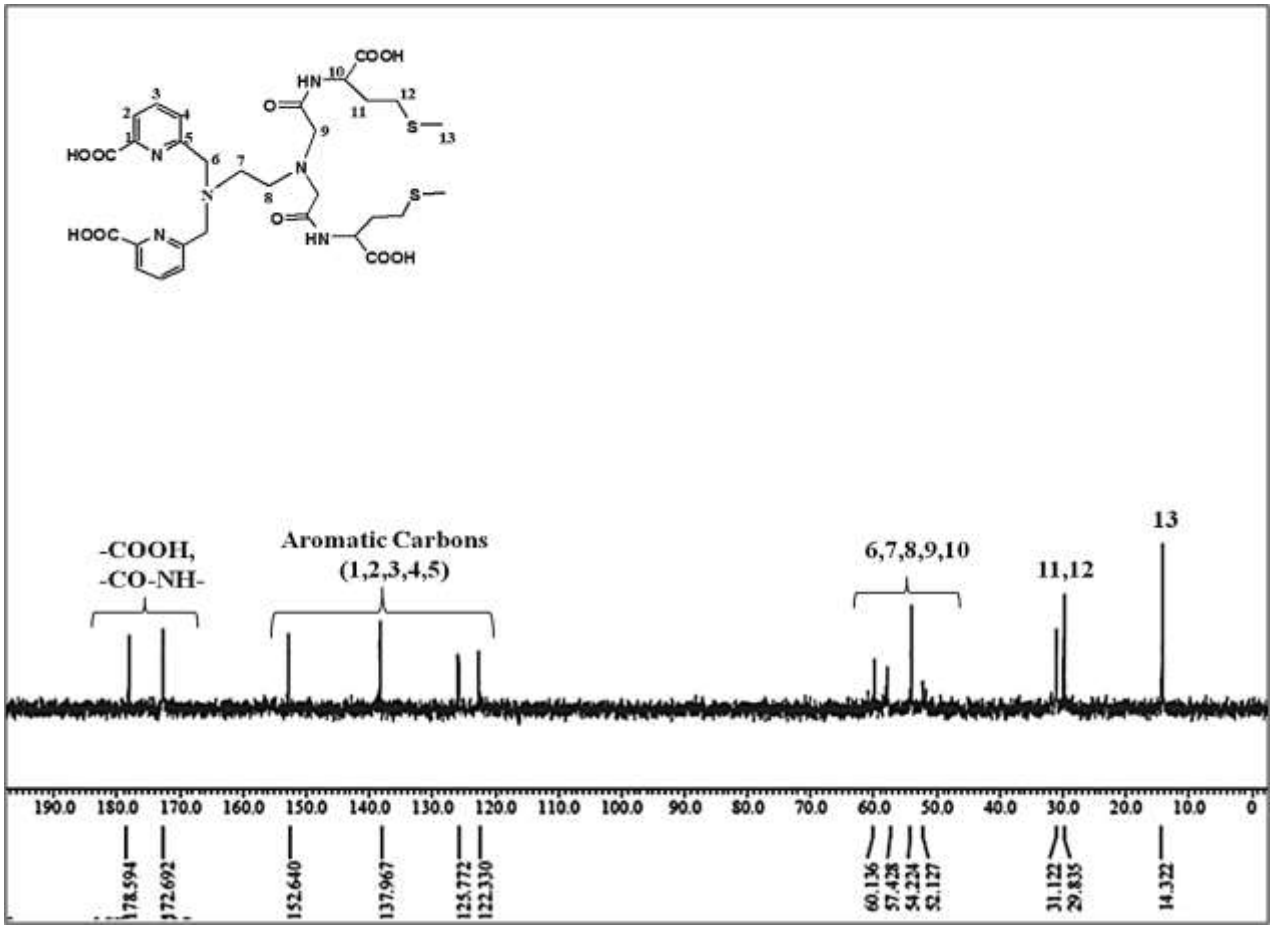

Figure S26. ^{13}C NMR spectrum of 6-(9-carboxy-5-(1-carboxy-3-(methylthio) propylamino)-2-oxoethyl)-2-((6-carboxypyridin-2-yl)methyl)-7-oxo-12thia-2,5,8-triazatridecyl)picolonic acid (**H_2pentapa-en-met$_2$**)

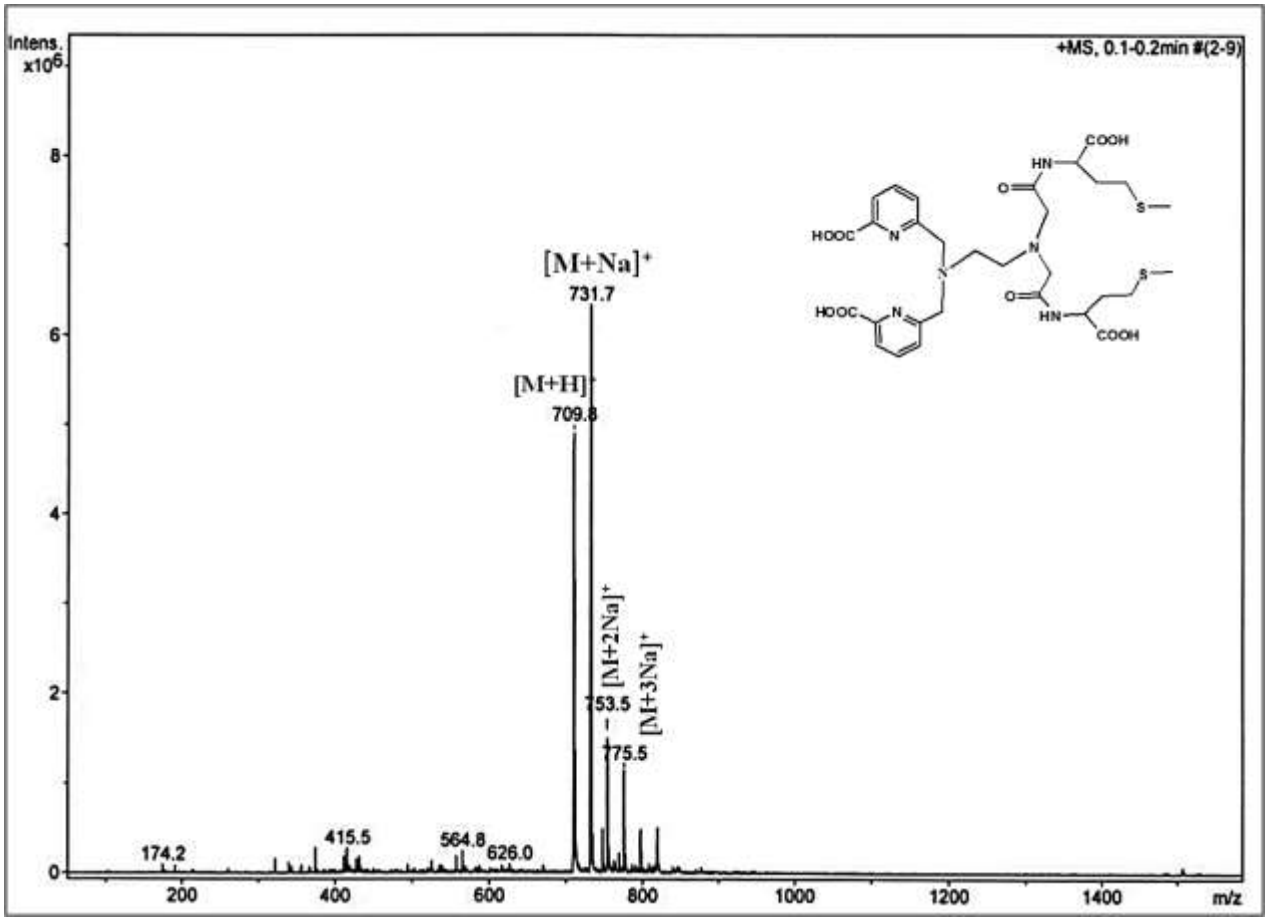

Figure S27. Mass spectrum of 6-(9-carboxy-5-(1-carboxy-3-(methylthio) propylamino)-2-oxoethyl)-2-((6-carboxypyridin-2-yl)methyl)-7-oxo-12thia-2,5,8-triazatridecyl)picolonic acid (**H_2pentapa-en-met$_2$**)

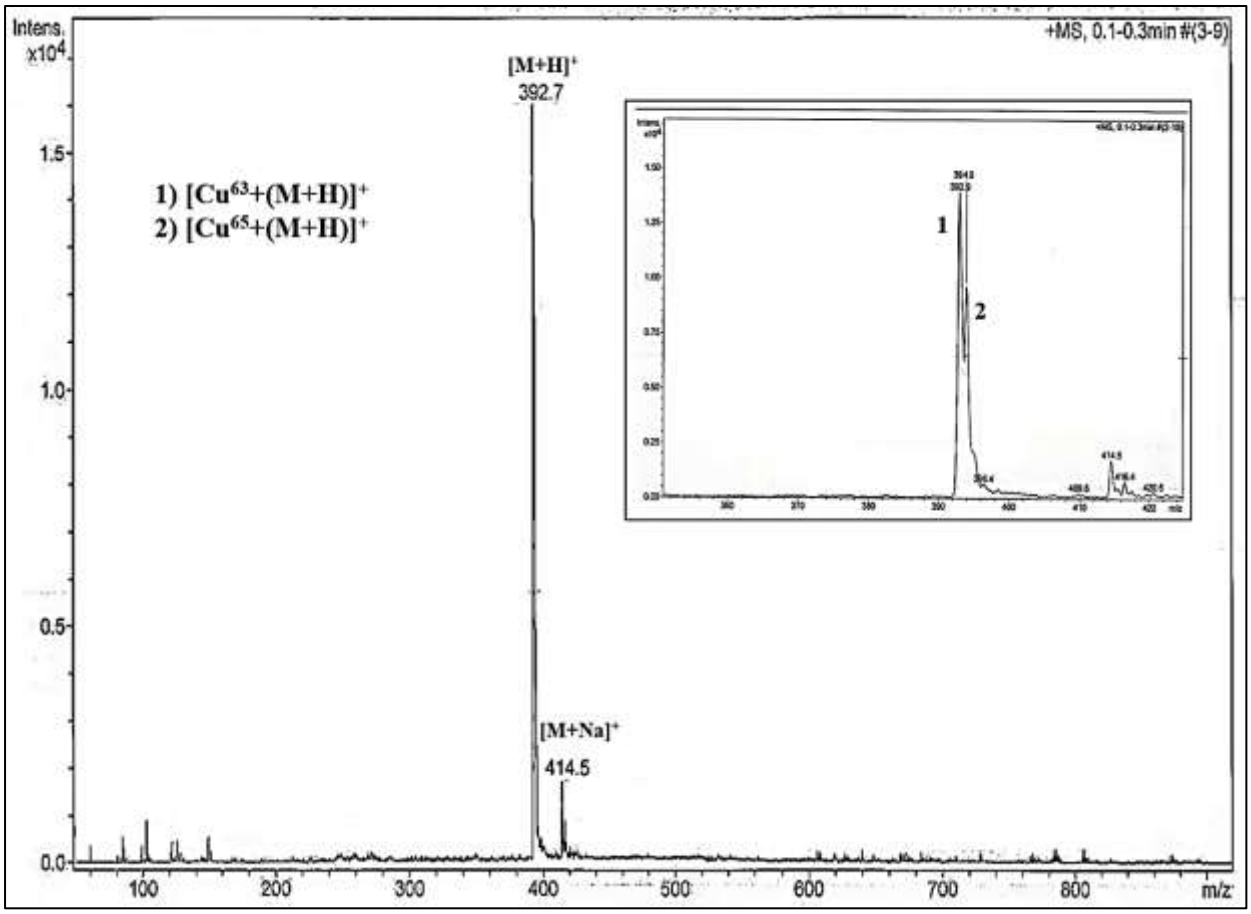

Figure S28. Mass spectrum of **Cu-H_2pentapa-en-NH_2**

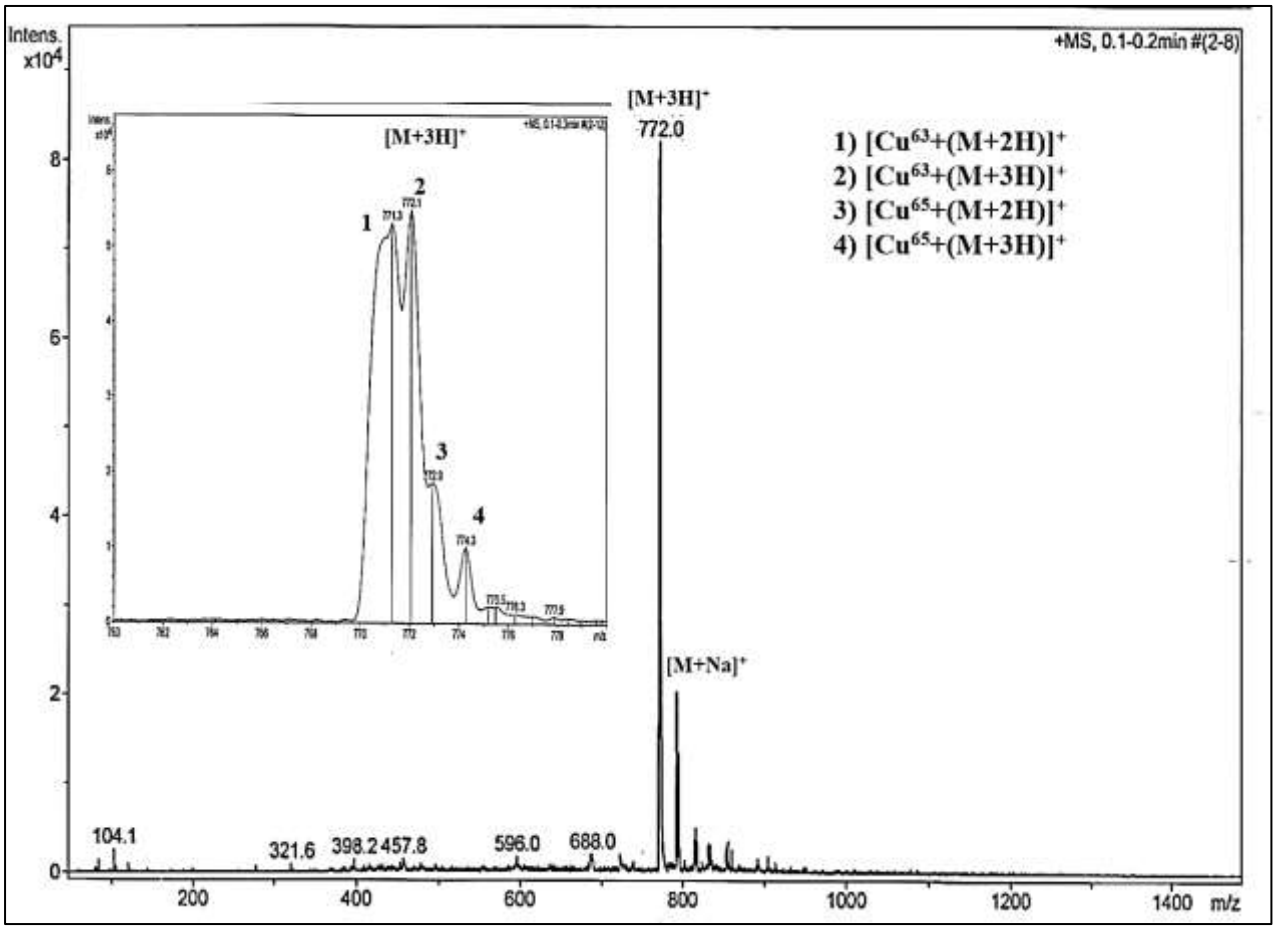

Figure S29. Mass spectrum of **Cu-H_2pentapa-en-met$_2$**

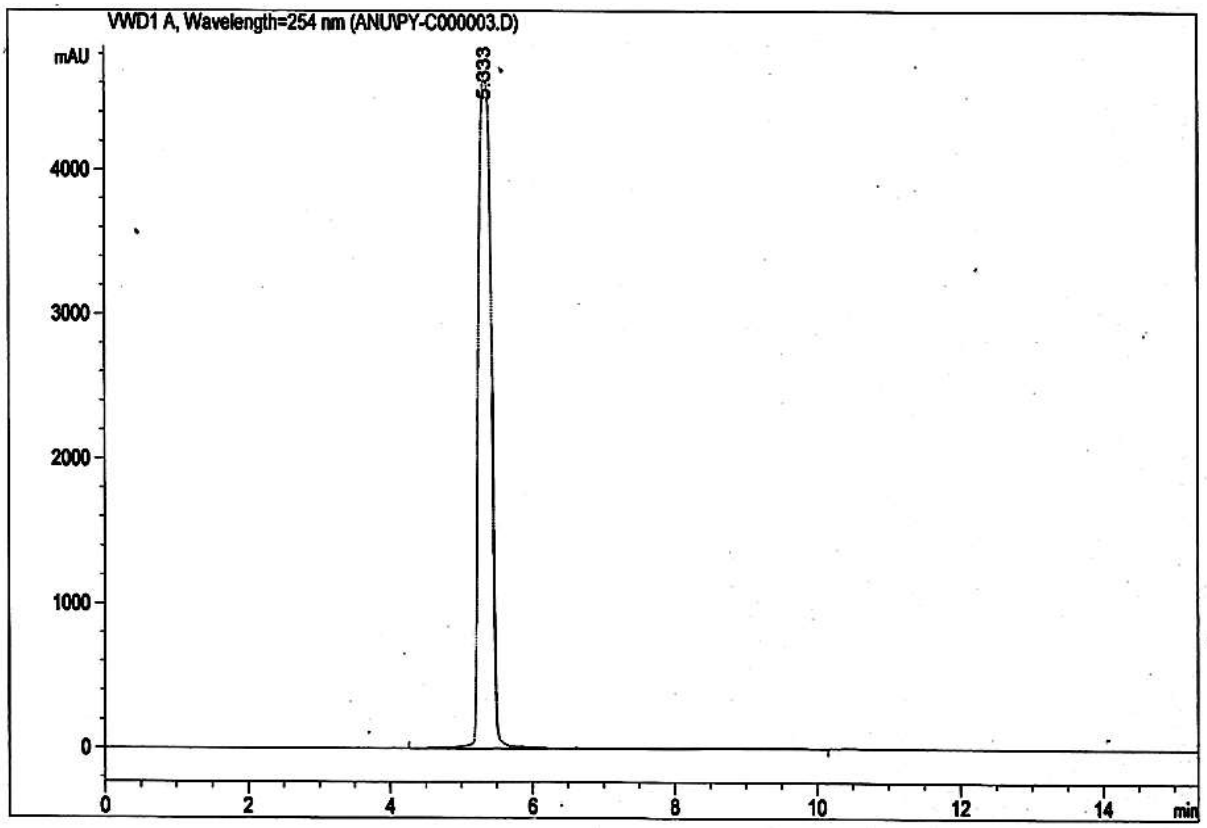

Figure S30. HPLC Profile of **H_2pentapa-en-NH_2**

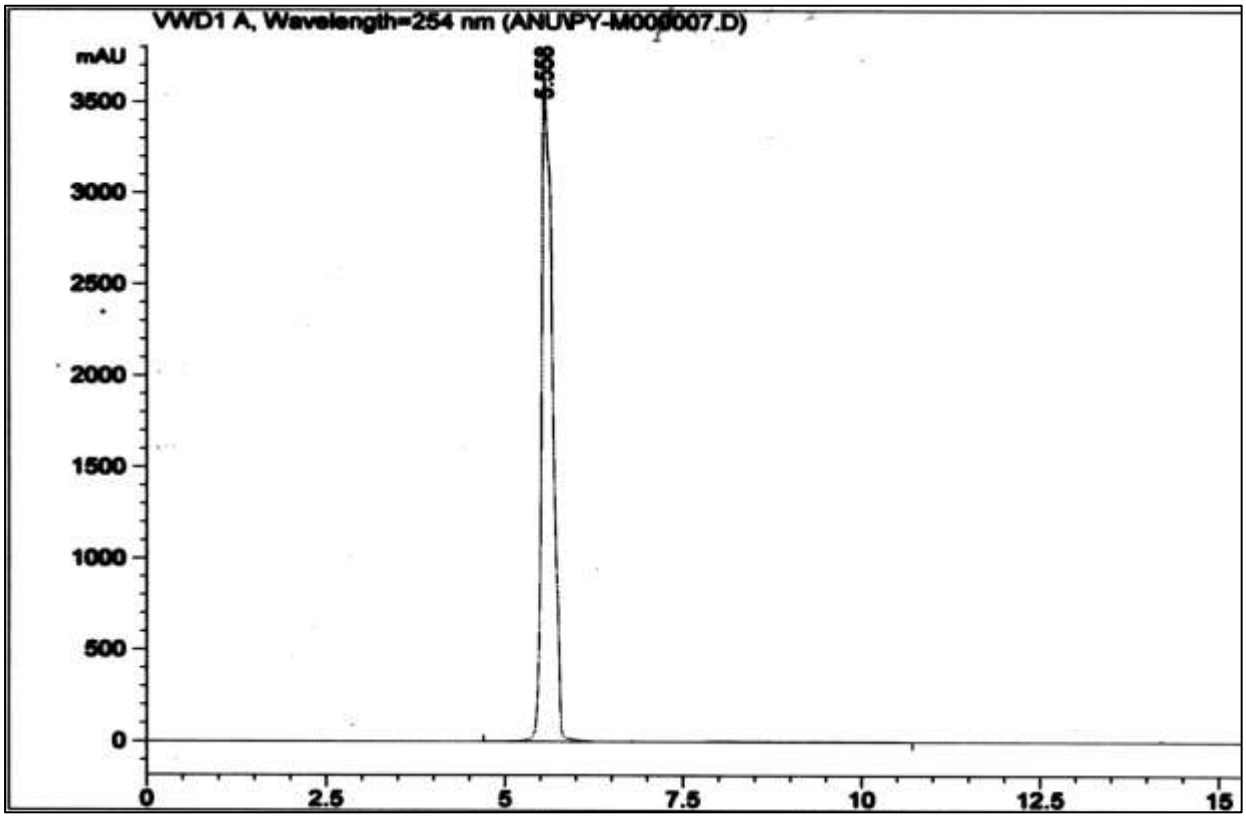

Figure S31. HPLC Profile of **H_2pentapa-en-met$_2$**

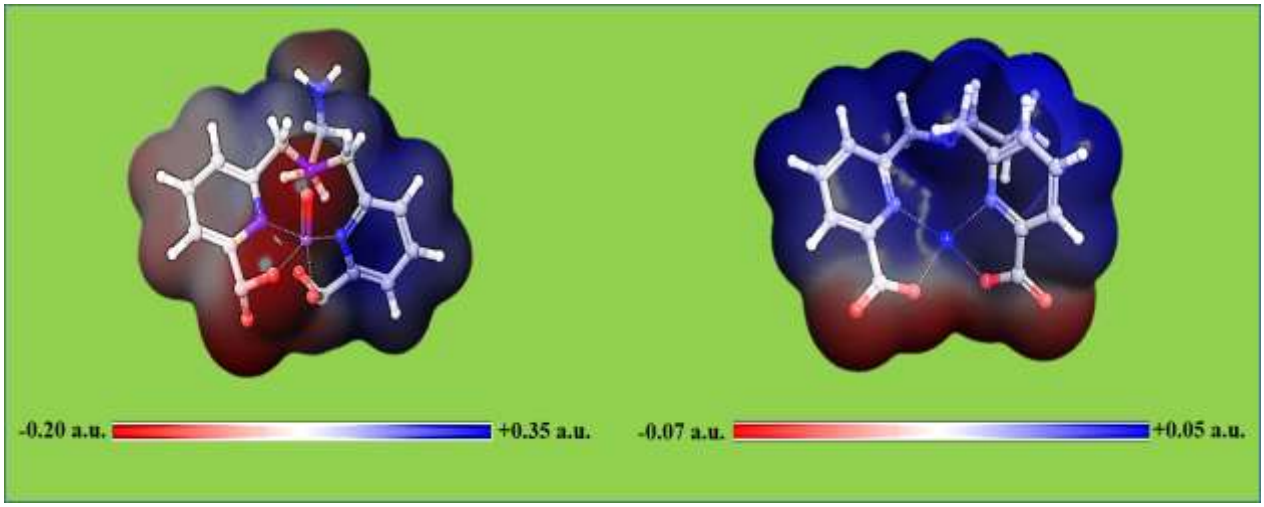

Figure S32. *In silico* DFT predicted electrostatic potential map of **[ReO(pentapa-en-NH_2)]$^+$** and **Cu-pentapa-en-NH_2** varying from -0.20 a.u. to +0.35 a.u. and -0.07 a.u. to +0.05 a.u. respectively

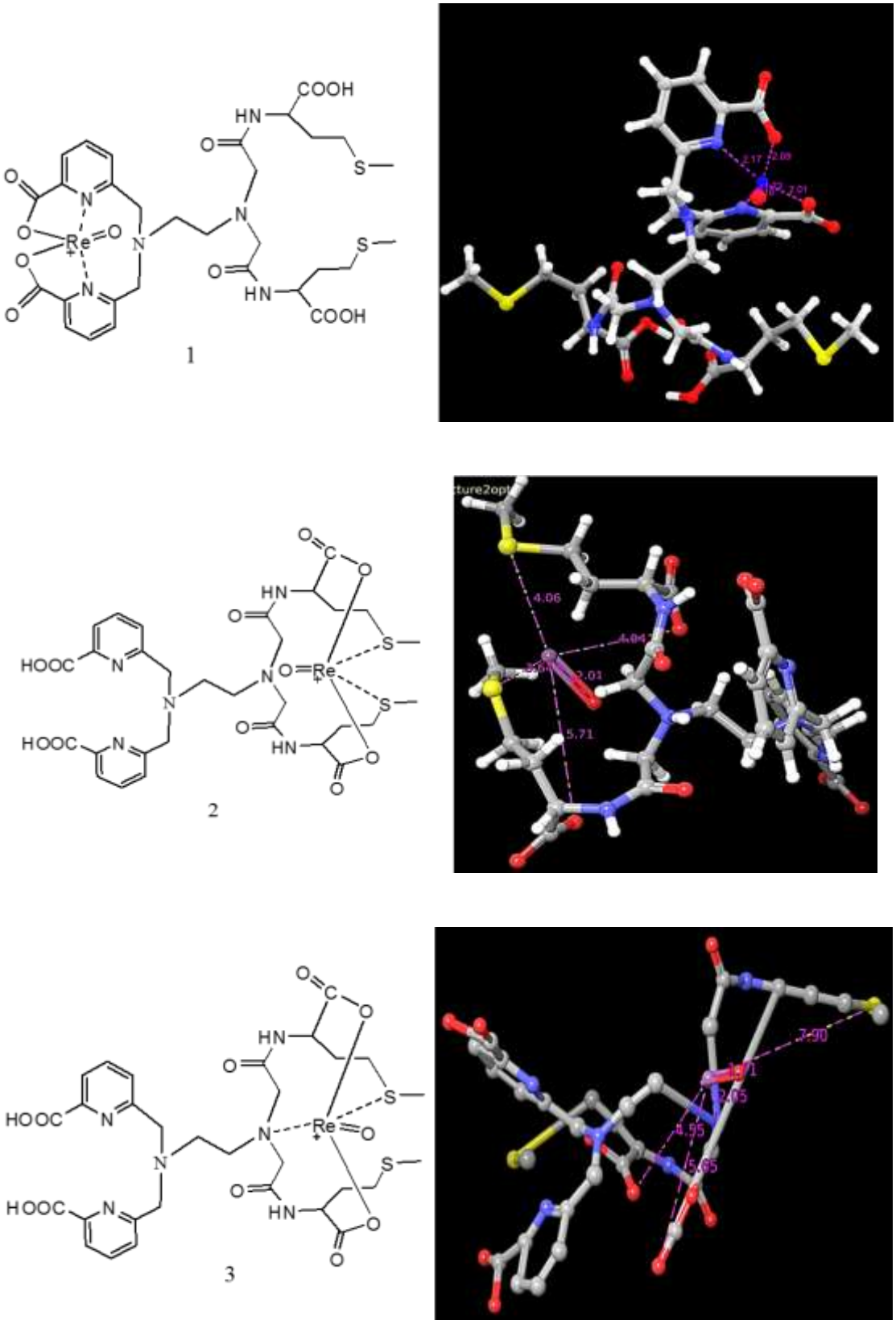

Figure S33. DFT studies showing the bond lengths after coordination of Rhenium oxocore to H_2pentapa-en-met_2

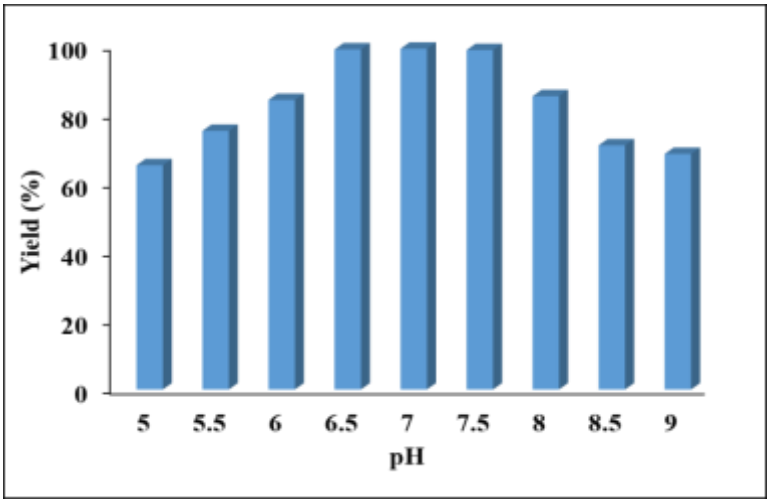

Figure S34. Effect of pH on radio chemical yield of H_2pentapa-en-NH_2 and H_2pentapa-en-met_2 with ^{99m}Tc

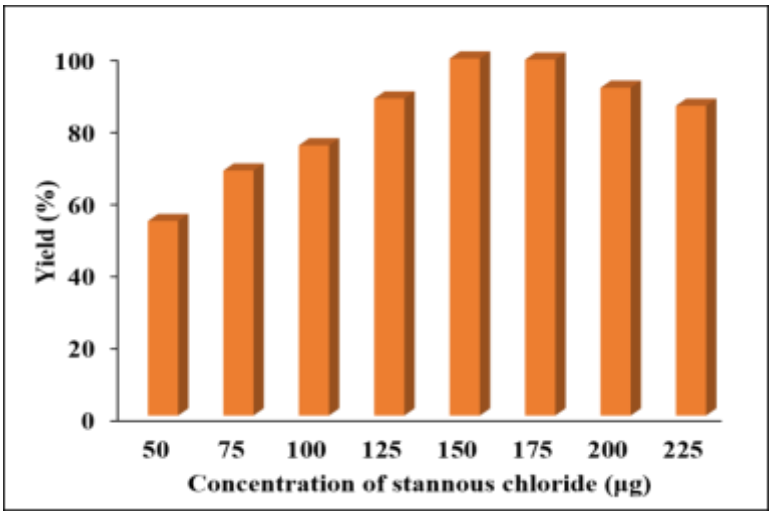

Figure S35. Effect of stannous chloride concentration on radio chemical yield of H_2pentapa-en-NH_2 and H_2pentapa-en-met_2 with ^{99m}Tc

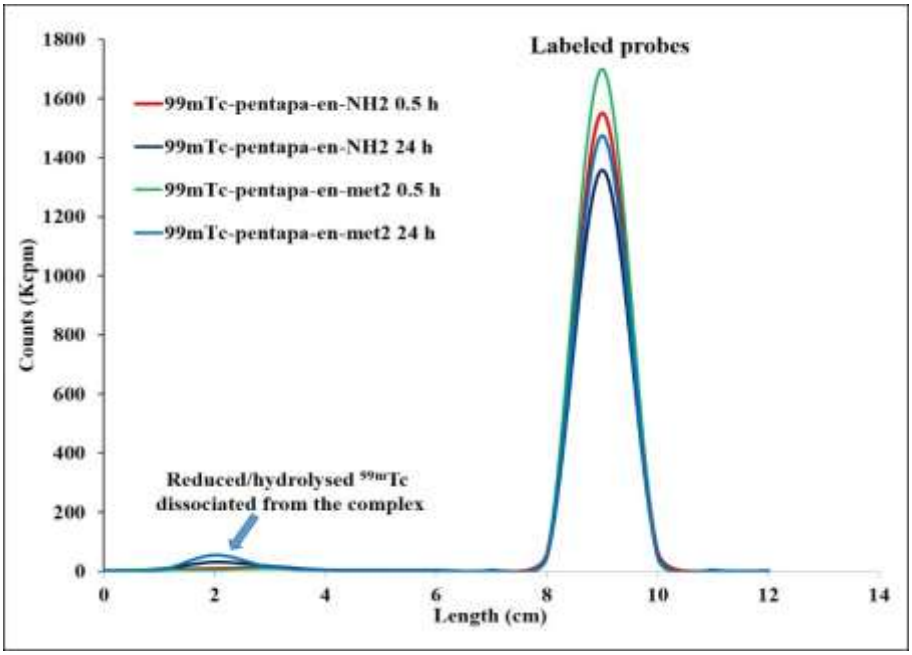

Figure S36. ITLC profile of ^{99m}Tc complexes of H_2pentapa-en-NH_2 and H_2pentapa-en-met_2 at various time intervals in PBS buffer using pyridine/acetic acid/water (3:5:1.5) as mobile phase

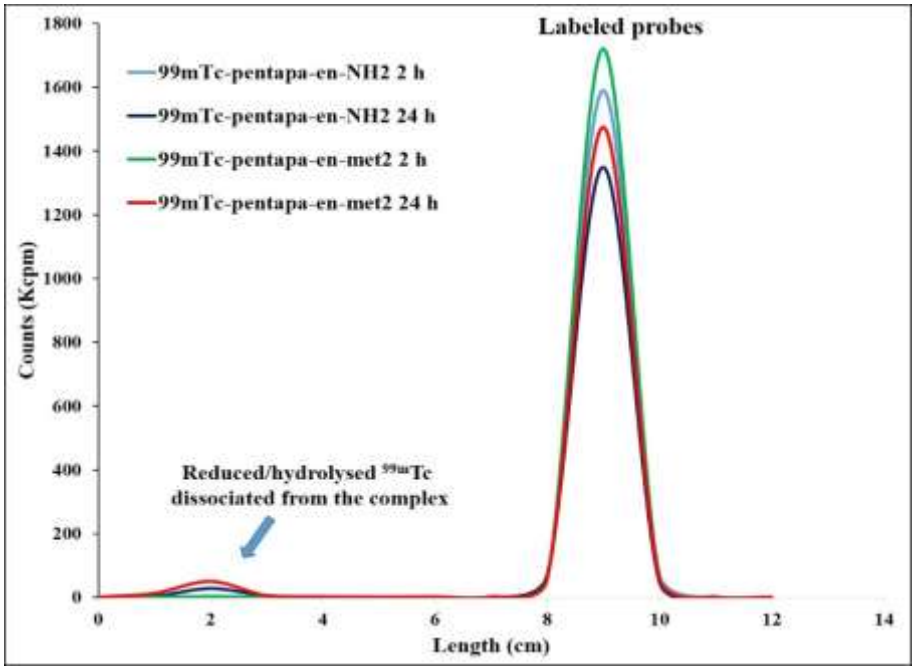

Figure S37. ITLC profile of ^{99m}Tc complexes of H_2pentapa-en-NH_2 and H_2pentapa-en-met_2 at various time intervals in human serum using pyridine/acetic acid/water (3:5:1.5) as mobile phase

Table S1. Comparison of bond lengths obtained through DFT studies after coordination of rhenium oxocore to penatapa-en-met$_2$ with bond lengths of reported XRD crystal structure of methionine conjugated rhenium oxocore.

	Re−O (Re=O)	Re−O (Re−O−C=O)	Re−N	Re-S
Met-Re [$ReOX_2$(Met)]	1.66 Å	2.05 Å	2.14 Å ($Re-NH_2$)	2.42 Å
ReO[penatapa-en-met$_2$]$^+$ (1)	1.72 Å	2.01 Å, 2.09 Å	2.16 Å, 2.17 Å	-
ReO[penatapa-en-met$_2$]$^+$ (2)	2.01 Å	4.04 Å, 5.71 Å	-	4.06 Å, 3.64 Å
ReO[penatapa-en-met$_2$]$^+$ (3)	1.71 Å	4.55 Å, 5.65 Å	2.65 Å	7.90 Å

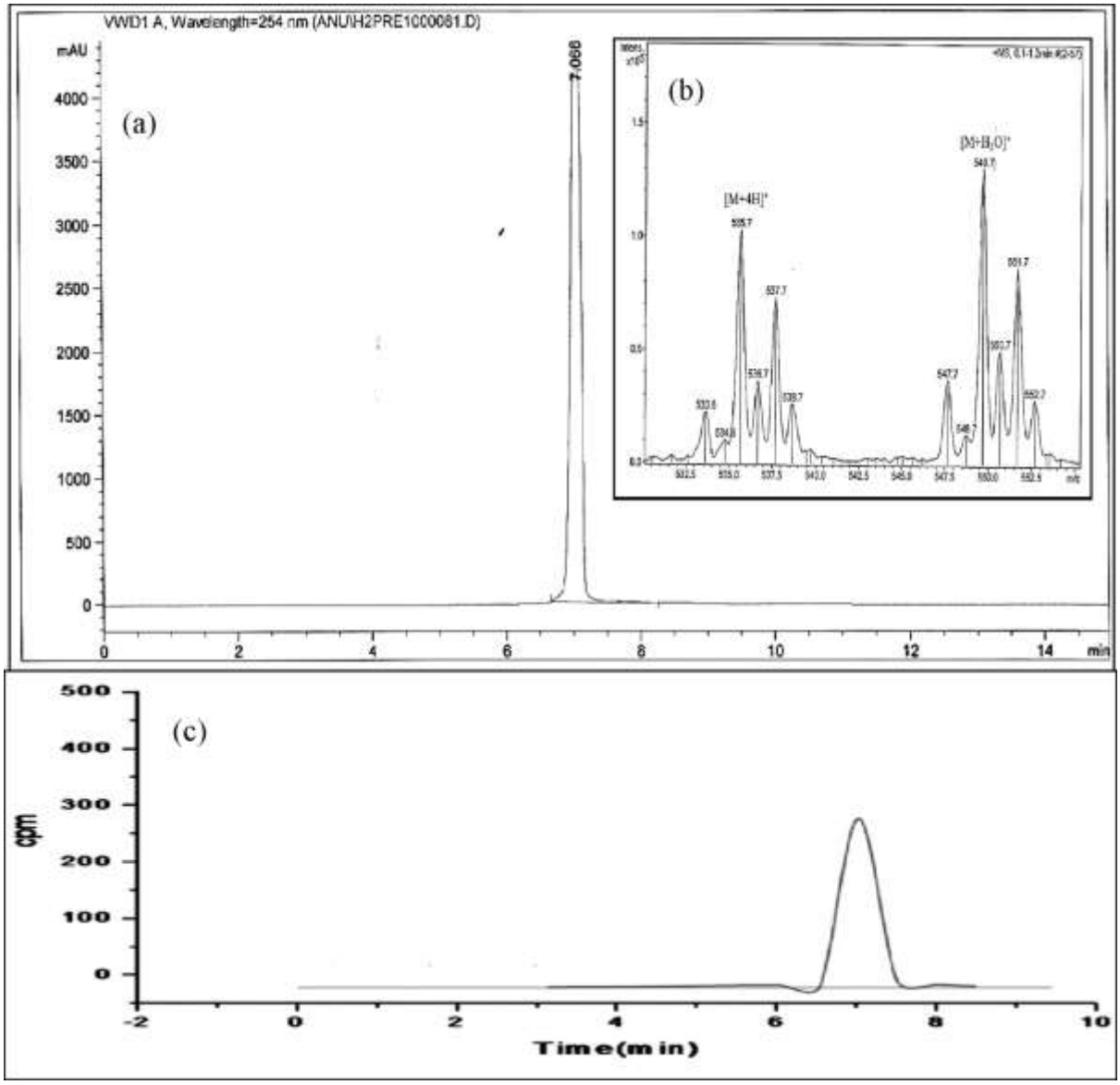

Figure S38. (a) HPLC profile and (b) mass spectrum of Re-pentapa-en-NH_2; (c) HPLC profile (γ- detector) of ^{99m}Tc-pentapa-en-NH_2

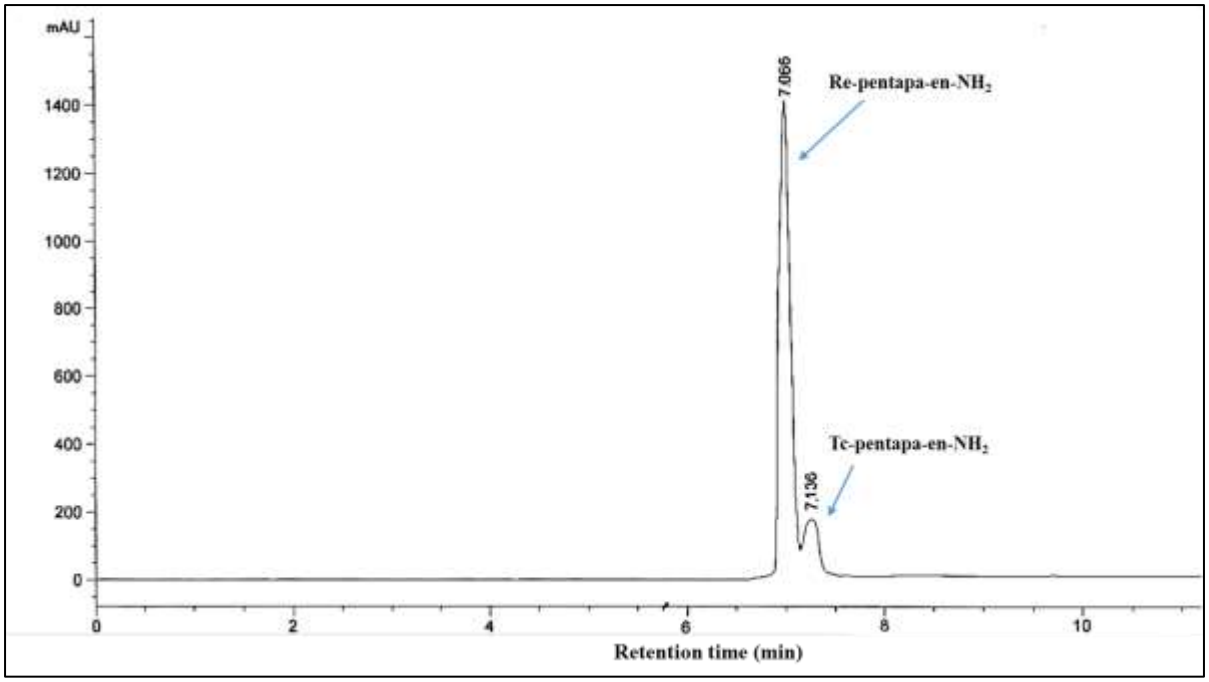

Figure S39. HPLC profile of co-injected metal complexes of Re-pentapa-en-NH_2 and Tc-pentapa-en-NH_2

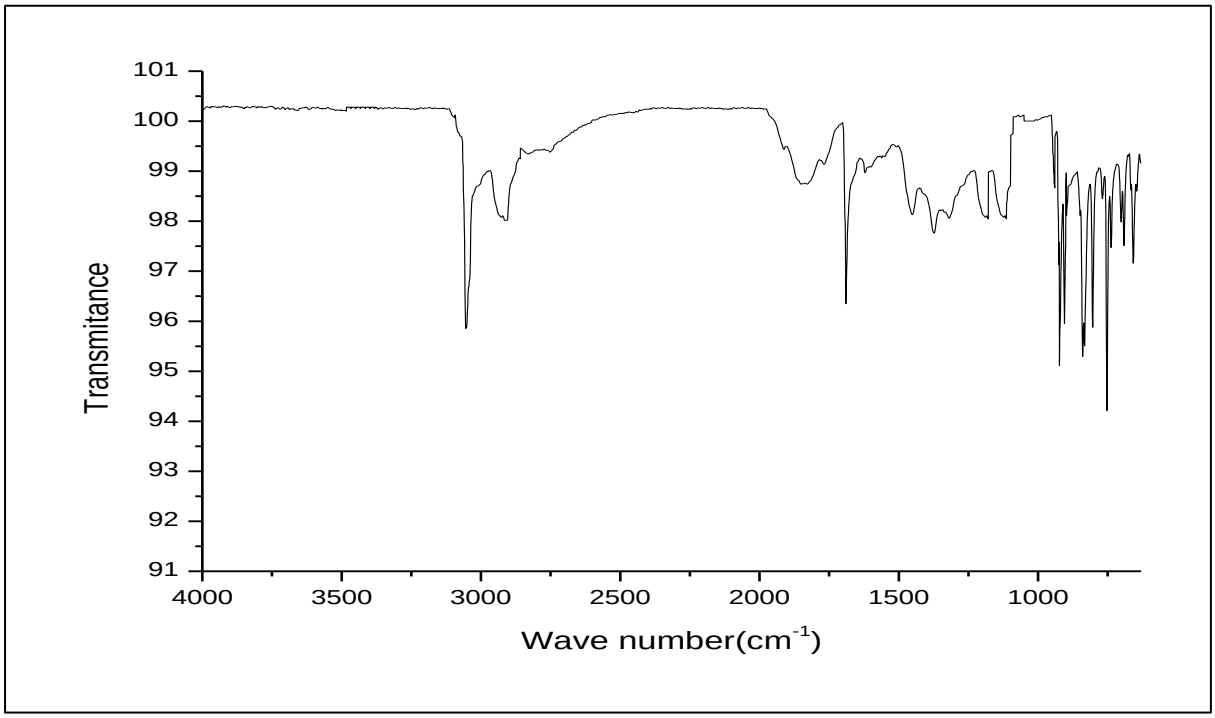

Figure S40. IR spectrum of Re-pentapa-en-NH_2